

Statistical anisotropy in galaxy ellipticity correlations

Maresuke Shiraishi,^a Teppei Okumura,^{b,c} and Kazuyuki Akitsu^d

^aSchool of General and Management Studies, Suwa University of Science, Chino, Nagano 391-0292, Japan

^bAcademia Sinica Institute of Astronomy and Astrophysics (ASIAA), No. 1, Section 4, Roosevelt Road, Taipei 10617, Taiwan

^cKavli Institute for the Physics and Mathematics of the Universe (WPI), UTIAS, The University of Tokyo, Chiba 277-8583, Japan

^dSchool of Natural Sciences, Institute for Advanced Study, 1 Einstein Drive, Princeton, NJ 08540, USA

E-mail: shiraishi_maresuke@rs.sus.ac.jp, tokumura@asiaa.sinica.edu.tw, kakitsu@ias.edu

Abstract. As well as the galaxy number density and peculiar velocity, the galaxy intrinsic alignment can be used to test the cosmic isotropy. We study distinctive impacts of the isotropy breaking on the configuration-space two-point correlation functions (2PCFs) composed of the spin-2 galaxy ellipticity field. For this purpose, we build a formalism for general types of the isotropy-violating 2PCFs and a methodology to efficiently compute them by generalizing the polypolar spherical harmonic decomposition approach to the spin-weighted version. As a demonstration, we analyze the 2PCFs when the matter power spectrum has a well-known g_* -type isotropy-breaking term (induced by, e.g., dark vector fields). We then confirm that some anisotropic distortions indeed appear in the 2PCFs and their shapes rely on a preferred direction causing the isotropy violation, \hat{d} . Such a feature can be a distinctive indicator for testing the cosmic isotropy. Comparing the isotropy-violating 2PCFs computed with and without the plane parallel (PP) approximation, we find that, depending on \hat{d} , the PP approximation is no longer valid when an opening angle between the directions towards target galaxies is $\mathcal{O}(1^\circ)$ for the density-ellipticity and velocity-ellipticity cross correlations and around 10° for the ellipticity auto correlation. This suggests that an accurate test for the cosmic isotropy requires the formulation of the 2PCF without relying on the PP approximation.

Contents

1	Introduction	1
2	Galaxy density, velocity and ellipticity fields induced by a general type of the isotropy-breaking matter fluctuation	2
2.1	Isotropy-breaking matter fluctuation	3
2.2	Spin-0 galaxy field: density δ and velocity u	4
2.3	Spin-2 galaxy field: ellipticity $\pm 2\gamma$	5
2.4	Unified form of the galaxy field	6
3	Efficient computation methodology for general types of the isotropy-breaking galaxy correlations	7
3.1	Isotropy-breaking galaxy correlations	7
3.2	Spin-weighted tripolar spherical harmonic decomposition approach for the exact analysis	8
3.3	Spin-weighted bipolar spherical harmonic decomposition approach for the plane-parallel-limit analysis	10
4	Correlations of the ellipticity field in the g_* model	12
5	Conclusions	16
A	Correlations of the density and velocity fields in the g_* model	17
B	Angular correlation functions	19
C	Useful mathematical identities	21

1 Introduction

Global isotropy of the Universe is a major conjecture in cosmology, and it has been supported by various types of the cosmic observations so far. However, the possibility of a small isotropy violation still has been allowed and forthcoming observations will reveal it.

Theoretically, the statistical isotropy of the Universe can be violated by the existence of strong anisotropic sources like vector fields. There are already various inflationary scenarios including vector fields motivated by, e.g., magnetogenesis and axiverse models (see e.g. refs. [1–3] for review). Behaviors of vector fields as dark matter and dark energy candidates have also been thoroughly argued (e.g. refs. [4–7]). Testing the statistical isotropy in cosmic observables therefore becomes a powerful diagnostic approach of such scenarios. The cosmic microwave background (CMB) observations have already tightly constrained the statistical isotropy breaking [8–10], and a bit weaker limits have been obtained via the measurement of the galaxy number density from galaxy surveys [11, 12].

Regarding observables in the galaxy surveys, not only conventional spin-0 fields that are number density and peculiar velocity,¹ but also a spin-2 field, ellipticity, have rich information

¹The peculiar velocity can also have a vorticity-induced spin-1 component, however, it is negligibly small in the standard cosmology.

and hence the galaxy ellipticity field has recently come into use as a beneficial cosmological probe (e.g. refs. [13–24]). Implementation of the ellipticity field in the isotropy test is naturally expected to improve the constraint or yield some novel information. Motivated by this, in this paper, we, for the first time, study distinctive impacts of the isotropy breaking on the configuration-space two-point correlation functions (2PCFs) composed of the ellipticity field. For this purpose, we develop a formalism for general types of the isotropy-violating 2PCFs and a methodology to efficiently compute them.

The technique of spin-weighted polypolar spherical harmonic (PolypoSH) decomposition can be used as a powerful tool to compute galaxy statistics including the intricate spin and angular dependence.² Using this technique, previous studies presented the analysis of wide-angle effects of spin-0 [29–36] and higher-spin [37] field correlations, and isotropy-breaking signatures of spin-0 field ones [38–41]. We here generalize the decomposition technique to deal with general types of isotropy-breaking signatures on higher-spin field correlations.

As a numerical application of this new methodology, we analyze the 2PCFs generated in the case where the matter power spectrum has a well-known g_* -type isotropy-breaking term [11, 42] induced by, e.g., dark vector fields (hereinafter called the g_* model). For the first step, we examine the plane-parallel (PP) limit, where an opening angle (dubbed as Θ) between two line-of-sight (LOS) directions toward the positions of galaxies, $\hat{x}_1 \equiv \mathbf{x}_1/x_1$ and $\hat{x}_2 \equiv \mathbf{x}_2/x_2$, is small enough that we can approximate $\hat{x}_1 \simeq \hat{x}_2 = \hat{x}_p$. Hence, the 2PCFs are computable using the spin-weighted bipolar spherical harmonic (BipoSH) basis, $\{Y_\ell(\hat{x}_{12}) \otimes_{\lambda'} Y_{\ell'}(\hat{x}_p)\}_{LM}$, where $\hat{x}_{12} \equiv (\mathbf{x}_1 - \mathbf{x}_2)/|\mathbf{x}_1 - \mathbf{x}_2|$ is the direction of the separation vector between the positions of target galaxies. Showing obtained 2PCF signals as a function of parallel and perpendicular elements of \mathbf{x}_{12} as in ref. [43], we find some distinctive distortions due to the isotropy breaking, which could be a key indicator for testing the cosmic isotropy.

The PP approximation would not be applicable to the analysis in futuristic wider galaxy surveys. Therefore, as the next step, we treat \hat{x}_1 and \hat{x}_2 separately, and compute the 2PCFs by introducing the spin-weighted tripolar spherical harmonic (TripoSH) basis $\{Y_\ell(\hat{x}_{12}) \otimes_{\lambda_1} Y_{\ell_1}(\hat{x}_1) \otimes_{\lambda_2} Y_{\ell_2}(\hat{x}_2)\}_{\ell' LM}$. Comparing the exact results with the PP-limit ones for the g_* model, we measure the error level of the PP approximation as a function of Θ . We then find that it is sensitive to a global preferred direction causing the isotropy violation and exceeds 10% up to $\Theta = \mathcal{O}(1^\circ)$ at worst, indicating the importance of beyond the PP-limit analysis for testing the cosmic isotropy more accurately.

This paper is organized as follows. In the next section, we derive a formalism on the galaxy density, velocity and ellipticity fields originating from a general type of the isotropy-breaking matter fluctuation. In section 3, we build an efficient computation methodology for general types of the isotropy-breaking 2PCFs with and without the PP approximation by means of the BipoSH and TripoSH techniques, respectively. Section 4 presents a numerical analysis of the 2PCFs in the g_* model, and the final section concludes this work.

2 Galaxy density, velocity and ellipticity fields induced by a general type of the isotropy-breaking matter fluctuation

For later analysis of the large-scale statistics, in this section, we derive a linear theory expressions of the galaxy density, velocity and ellipticity fields when the underlying matter fluctuation breaks isotropy in a general way.

²For different but similar approaches, see refs. [25–28].

2.1 Isotropy-breaking matter fluctuation

In the following analysis, we impose the statistical homogeneity of the real-space matter fluctuation $\delta_{\mathbf{m}}$; thus, the matter power spectrum generally takes the form

$$\langle \delta_{\mathbf{m}}(\mathbf{k}_1) \delta_{\mathbf{m}}(\mathbf{k}_2) \rangle = (2\pi)^3 \delta^{(3)}(\mathbf{k}_1 + \mathbf{k}_2) P_{\mathbf{m}}(\mathbf{k}_1). \quad (2.1)$$

As we are in position to consider the statistical isotropy violation of $\delta_{\mathbf{m}}$, the \hat{k} dependence remains in $P_{\mathbf{m}}(\mathbf{k})$. We also assume the Gaussianity of $\delta_{\mathbf{m}}$ and therefore may ignore any impact of higher-order statistics. Here, although $\delta_{\mathbf{m}}$ depends on time, redshift or the comoving distance, it is not explicitly stated as an argument for notational convenience. This convention is adapted to all variables henceforth unless the parameter dependence is nontrivial and the explicit representation is needed.

Without loss of generality, we can expand $P_{\mathbf{m}}(\mathbf{k})$ according to

$$\begin{aligned} P_{\mathbf{m}}(\mathbf{k}) &= \bar{P}_{\mathbf{m}}(k) \left[1 + \sum_{L>0} \sum_M G_{LM}(k) Y_{LM}(\hat{k}) \right] \\ &= \bar{P}_{\mathbf{m}}(k) \sum_{LM} G_{LM}(k) Y_{LM}(\hat{k}), \end{aligned} \quad (2.2)$$

where $G_{LM}^* = (-1)^M G_{L,-M}$ and $G_{L=\text{odd},M} = 0$. Breaking the statistical isotropy gives rise to nonvanishing $G_{L>0,M}$. On the other hand, we define $G_{00} \equiv \sqrt{4\pi}$, so that $P_{\mathbf{m}}(\mathbf{k}) = \bar{P}_{\mathbf{m}}(k)$ holds if $\delta_{\mathbf{m}}$ is statistically isotropic. Because of observational bounds as $|G_{L>0,M}| \ll 1$, the matter density field satisfying eq. (2.2) takes the form

$$\delta_{\mathbf{m}}(\mathbf{k}) = \bar{\delta}_{\mathbf{m}}(\mathbf{k}) \left[1 + \frac{1}{2} \sum_{L>0} \sum_M G_{LM}(k) Y_{LM}(\hat{k}) \right], \quad (2.3)$$

where $\bar{\delta}_{\mathbf{m}}$ denotes the isotropy-conserving part in the matter fluctuation, whose power spectrum is given by

$$\langle \bar{\delta}_{\mathbf{m}}(\mathbf{k}_1) \bar{\delta}_{\mathbf{m}}(\mathbf{k}_2) \rangle = (2\pi)^3 \delta^{(3)}(\mathbf{k}_1 + \mathbf{k}_2) \bar{P}_{\mathbf{m}}(k_1). \quad (2.4)$$

Let us also introduce another mathematically-equivalent representation:

$$\begin{aligned} P_{\mathbf{m}}(\mathbf{k}) &= \bar{P}_{\mathbf{m}}(k) \left[1 + \mathcal{G}_{ij}^{(2)}(k) \hat{k}_i \hat{k}_j + \mathcal{G}_{ijkl}^{(4)}(k) \hat{k}_i \hat{k}_j \hat{k}_k \hat{k}_l + \mathcal{G}_{ijklmn}^{(6)}(k) \hat{k}_i \hat{k}_j \hat{k}_k \hat{k}_l \hat{k}_m \hat{k}_n + \dots \right] \\ &= \bar{P}_{\mathbf{m}}(k) \left[1 + \sum_{L>0} \mathcal{G}_{i_1 \dots i_L}^{(L)}(k) \prod_{r=1}^L \hat{k}_{i_r} \right], \end{aligned} \quad (2.5)$$

where $\mathcal{G}_{i_1 \dots i_L}^{(L)}$ is a totally symmetric rank- L traceless tensor field obeying $\mathcal{G}_{i_1 \dots i_L}^{(L)} \in \mathbb{R}$ and $\mathcal{G}_{i_1 \dots i_L}^{(L=\text{odd})} = 0$. In this expression, nonvanishing $\mathcal{G}_{i_1 \dots i_L}^{(L)}$ fully characterize isotropy-breaking signatures. Observational bounds as $|\mathcal{G}_{i_1 \dots i_L}^{(L)}| \ll 1$ lead to

$$\delta_{\mathbf{m}}(\mathbf{k}) = \bar{\delta}_{\mathbf{m}}(\mathbf{k}) \left[1 + \frac{1}{2} \sum_{L>0} \mathcal{G}_{i_1 \dots i_L}^{(L)}(k) \prod_{r=1}^L \hat{k}_{i_r} \right]. \quad (2.6)$$

In the remainder of this section, we first derive the linear theory formulae with the later tensorial representation, and finally rewrite them using the former harmonic one for good compatibility with the PolypoSH decomposition performed in the next section. We then utilize the conversion formulae:

$$\begin{aligned}
G_{LM}(k) &= \int d^2\hat{k} Y_{LM}^*(\hat{k}) \mathcal{G}_{i_1 \dots i_L}^{(L)}(k) \prod_{r=1}^L \hat{k}_{i_r}, \\
\mathcal{G}_{i_1 \dots i_L}^{(L)}(k) &= \frac{(2L+1)!!}{4\pi L!} \int d^2\hat{k} \left(\prod_{r=1}^L \hat{k}_{i_r} \right) \sum_M G_{LM}(k) Y_{LM}(\hat{k}),
\end{aligned} \tag{2.7}$$

where the latter one has been derived employing eq. (C.6).

2.2 Spin-0 galaxy field: density δ and velocity u

Here we formulate the number density fluctuation, $\delta(\mathbf{x}) \equiv n(\mathbf{x})/n_{\text{av}}(x) - 1$, and the LOS component of peculiar velocity, $u(\mathbf{x}) \equiv \mathbf{v}(\mathbf{x}) \cdot \hat{x}$, in the redshift space.

As shown in eq. (2.6), the real-space matter density field δ_{m} is anisotropically modulated by some extra tensor field $\mathcal{G}_{i_1 \dots i_L}^{(L)}$ (and hence the isotropy-breaking matter power spectrum (2.5) is realized). Such a field could also give characteristic impacts on the bias relation between galaxy and matter number densities [14, 19]. In a similar manner to refs. [14, 19, 44], we fully expand the real-space galaxy number density field δ^r with respect to $\frac{\partial_i \partial_j}{\partial^2} \delta_{\text{m}}$ by using the Kronecker delta δ_{ij}^{K} and $\mathcal{G}_{i_1 \dots i_L}^{(L)}$ for tensor contractions. We then find that δ^r at leading order of δ_{m} is expressed with two different bias parameters b_{g} and $b_{\text{g}}^{(2)}$; namely,

$$\delta^r(\mathbf{x}) = \int \frac{d^3k}{(2\pi)^3} e^{i\mathbf{k}\cdot\mathbf{x}} \left[b_{\text{g}} + \frac{1}{2} b_{\text{g}}^{(2)} \mathcal{G}_{ij}^{(2)}(k) \hat{k}_i \hat{k}_j \right] \delta_{\text{m}}(\mathbf{k}). \tag{2.8}$$

Here, b_{g} is equivalent to a linear bias parameter introduced in standard isotropy-conserving universe models, while $b_{\text{g}}^{(2)}$ is a newly-introduced one due to nonvanishing $\mathcal{G}_{ij}^{(2)}$, or equivalently, nonvanishing G_{2M} . If moving to the redshift space, the usual distortion terms are added in this expression. Evaluation up to linear order of $\mathcal{G}_{i_1 \dots i_L}^{(L)}$ with eq. (2.6) yields

$$\begin{aligned}
\delta(\mathbf{x}) &= \bar{\delta}(\mathbf{x}) + \delta_{\text{ani}}^{\text{std}}(\mathbf{x}) + \delta_{\text{ani}}^{\text{new}}(\mathbf{x}), \\
\bar{\delta}(\mathbf{x}) &\equiv \int \frac{d^3k}{(2\pi)^3} e^{i\mathbf{k}\cdot\mathbf{x}} \left[b_{\text{g}} - i \frac{\alpha f}{kx} (\hat{k} \cdot \hat{x}) + f (\hat{k} \cdot \hat{x})^2 \right] \bar{\delta}_{\text{m}}(\mathbf{k}), \\
\delta_{\text{ani}}^{\text{std}}(\mathbf{x}) &\equiv \int \frac{d^3k}{(2\pi)^3} e^{i\mathbf{k}\cdot\mathbf{x}} \left[b_{\text{g}} - i \frac{\alpha f}{kx} (\hat{k} \cdot \hat{x}) + f (\hat{k} \cdot \hat{x})^2 \right] \left[\frac{1}{2} \sum_{L>0} \mathcal{G}_{i_1 \dots i_L}^{(L)}(k) \prod_{r=1}^L \hat{k}_{i_r} \right] \bar{\delta}_{\text{m}}(\mathbf{k}), \\
\delta_{\text{ani}}^{\text{new}}(\mathbf{x}) &\equiv \int \frac{d^3k}{(2\pi)^3} e^{i\mathbf{k}\cdot\mathbf{x}} \frac{1}{2} b_{\text{g}}^{(2)} \mathcal{G}_{ij}^{(2)}(k) \hat{k}_i \hat{k}_j \bar{\delta}_{\text{m}}(\mathbf{k}),
\end{aligned} \tag{2.9}$$

where f is the linear growth rate, a is the scale factor, H is the Hubble parameter, and $\alpha \equiv d \ln n_{\text{av}}(x) / d \ln x + 2$ is the selection function of a given galaxy sample. We note that $\bar{\delta}$ corresponds to the isotropy-conserving component, and $\delta_{\text{ani}}^{\text{std}}$ and $\delta_{\text{ani}}^{\text{new}}$ denote the isotropy-breaking ones depending on b_{g} and $b_{\text{g}}^{(2)}$, respectively. Taking $f \rightarrow 0$ in eq. (2.9) yields the representation of δ^r up to linear order of $\mathcal{G}_{i_1 \dots i_L}^{(L)}$.

In contrast, the velocity field is free from the above bias effect and therefore reads

$$\begin{aligned}
u(\mathbf{x}) &= \bar{u}(\mathbf{x}) + u_{\text{ani}}^{\text{std}}(\mathbf{x}) + u_{\text{ani}}^{\text{new}}(\mathbf{x}), \\
\bar{u}(\mathbf{x}) &\equiv \int \frac{d^3k}{(2\pi)^3} e^{i\mathbf{k}\cdot\mathbf{x}} i \frac{aHf}{k} (\hat{k} \cdot \hat{x}) \bar{\delta}_{\text{m}}(\mathbf{k}), \\
u_{\text{ani}}^{\text{std}}(\mathbf{x}) &\equiv \int \frac{d^3k}{(2\pi)^3} e^{i\mathbf{k}\cdot\mathbf{x}} i \frac{aHf}{k} (\hat{k} \cdot \hat{x}) \left[\frac{1}{2} \sum_{L>0} \mathcal{G}_{i_1 \dots i_L}^{(L)}(k) \prod_{r=1}^L \hat{k}_{i_r} \right] \bar{\delta}_{\text{m}}(\mathbf{k}), \\
u_{\text{ani}}^{\text{new}}(\mathbf{x}) &\equiv 0.
\end{aligned} \tag{2.10}$$

Regarding the velocity field, up to linear order of $\bar{\delta}_{\text{m}}$, the real-space expression coincides with this redshift-space one [45].

2.3 Spin-2 galaxy field: ellipticity $\pm 2\gamma$

The ellipticity field, γ_{ij} , is defined as the transverse and traceless projection of the second moment of the surface brightness of galaxies g_{ij}^I [see eq. (2.16)], namely,

$$\gamma_{ij}(\mathbf{x}) = \frac{1}{2} [P_{ik}(\hat{x})P_{jl}(\hat{x}) + P_{il}(\hat{x})P_{jk}(\hat{x}) - P_{ij}(\hat{x})P_{kl}(\hat{x})] g_{kl}^I(\mathbf{x}), \tag{2.11}$$

where $P_{ij}(\hat{x}) \equiv \delta_{ij}^{\text{K}} - \hat{x}_i \hat{x}_j$. A conventionally-used $+/ \times$ state is defined as

$$\begin{pmatrix} \gamma_+ \\ \gamma_\times \end{pmatrix}(\mathbf{x}) \equiv \begin{pmatrix} \hat{\theta}_i(\hat{x})\hat{\theta}_j(\hat{x}) - \hat{\phi}_i(\hat{x})\hat{\phi}_j(\hat{x}) \\ \hat{\theta}_i(\hat{x})\hat{\phi}_j(\hat{x}) + \hat{\phi}_i(\hat{x})\hat{\theta}_j(\hat{x}) \end{pmatrix} \gamma_{ij}(\mathbf{x}), \tag{2.12}$$

where $\hat{x} \equiv (\sin \theta \cos \phi, \sin \theta \sin \phi, \cos \theta)$, $\hat{\theta}(\hat{x}) \equiv (\cos \theta \cos \phi, \cos \theta \sin \phi, -\sin \theta)$ and $\hat{\phi}(\hat{x}) \equiv (-\sin \phi, \cos \phi, 0)$ are three orthonormal vectors. Here, for good compatibility with the later PolypoSH decomposition, we also introduce a helicity ± 2 state as

$$\pm 2\gamma(\mathbf{x}) \equiv m_{\mp}^i(\hat{x})m_{\mp}^j(\hat{x})\gamma_{ij}(\mathbf{x}), \tag{2.13}$$

where the polarization vector, given by

$$\mathbf{m}_{\pm}(\hat{x}) \equiv \frac{1}{\sqrt{2}} \left[\hat{\theta}(\hat{x}) \mp i\hat{\phi}(\hat{x}) \right], \tag{2.14}$$

obeys $\hat{x} \cdot \mathbf{m}_{\pm}(\hat{x}) = 0$, $\mathbf{m}_{\pm}^*(\hat{x}) = \mathbf{m}_{\mp}(\hat{x}) = \mathbf{m}_{\pm}(-\hat{x})$ and $\mathbf{m}_{\lambda}(\hat{x}) \cdot \mathbf{m}_{\lambda'}(\hat{x}) = \delta_{\lambda, -\lambda'}^{\text{K}}$. These two different states are linearly connected to each other and hence

$$\pm 2\gamma(\mathbf{x}) = \frac{1}{2} [\gamma_+(\mathbf{x}) \pm i\gamma_\times(\mathbf{x})]. \tag{2.15}$$

Similarly to the spin-0 case, $\mathcal{G}_{i_1 \dots i_L}^{(L)}$ is likely to affect the bias relation between δ_{m} and g_{ij}^I (and hence $\pm 2\gamma$). Fully expanding g_{ij}^I in terms of $\frac{\partial_i \partial_j}{\partial^2} \delta_{\text{m}}$ by use of δ_{ij}^{K} and $\mathcal{G}_{i_1 \dots i_L}^{(L)}$ for tensor contractions, we find the expression at linear order of δ_{m} :

$$\begin{aligned}
g_{ij}^I(\mathbf{x}) &= \int \frac{d^3k}{(2\pi)^3} e^{i\mathbf{k}\cdot\mathbf{x}} \left[b_{\text{K}} \left(\hat{k}_i \hat{k}_j - \frac{1}{3} \delta_{ij}^{\text{K}} \right) + \frac{1}{2} b_{\text{K}}^{(2,0)} \mathcal{G}_{ij}^{(2)}(k) \right. \\
&\quad \left. + \frac{1}{4} b_{\text{K}}^{(2,2)} \left(\mathcal{G}_{il}^{(2)}(k) \hat{k}_l \hat{k}_j + \mathcal{G}_{jl}^{(2)}(k) \hat{k}_l \hat{k}_i - \frac{2}{3} \mathcal{G}_{kl}^{(2)}(k) \hat{k}_k \hat{k}_l \delta_{ij}^{\text{K}} - \frac{2}{3} \mathcal{G}_{ij}^{(2)}(k) \right) \right. \\
&\quad \left. + \frac{1}{2} b_{\text{K}}^{(4)} \mathcal{G}_{ijkl}^{(4)}(k) \hat{k}_k \hat{k}_l \right] \delta_{\text{m}}(\mathbf{k}),
\end{aligned} \tag{2.16}$$

where b_K is equivalent to a linear bias parameter introduced in standard isotropy-conserving universe models, while the other three, $b_K^{(2,0)}$, $b_K^{(2,2)}$ and $b_K^{(4)}$, are newly-introduced ones due to nonvanishing $\mathcal{G}_{ij}^{(2)}$ and $\mathcal{G}_{ijkl}^{(4)}$, or equivalently, nonvanishing G_{2M} and G_{4M} . Converting this g_{ij}^I into the spin-2 field $\pm 2\gamma$ following the above conventions leads to the representation up to linear order of $\mathcal{G}_{i_1 \dots i_L}^{(L)}$:

$$\begin{aligned}
\pm 2\gamma(\mathbf{x}) &= \pm 2\bar{\gamma}(\mathbf{x}) + \pm 2\gamma_{\text{ani}}^{\text{std}}(\mathbf{x}) + \pm 2\gamma_{\text{ani}}^{\text{new}}(\mathbf{x}), \\
\pm 2\bar{\gamma}(\mathbf{x}) &\equiv \int \frac{d^3k}{(2\pi)^3} e^{i\mathbf{k}\cdot\mathbf{x}} b_K \hat{k}_i \hat{k}_j m_i^{\mp}(\hat{x}) m_j^{\mp}(\hat{x}) \bar{\delta}_{\mathbf{m}}(\mathbf{k}), \\
\pm 2\gamma_{\text{ani}}^{\text{std}}(\mathbf{x}) &\equiv \int \frac{d^3k}{(2\pi)^3} e^{i\mathbf{k}\cdot\mathbf{x}} b_K \hat{k}_i \hat{k}_j m_i^{\mp}(\hat{x}) m_j^{\mp}(\hat{x}) \left[\frac{1}{2} \sum_{L>0} \mathcal{G}_{i_1 \dots i_L}^{(L)}(k) \prod_{r=1}^L \hat{k}_{i_r} \right] \bar{\delta}_{\mathbf{m}}(\mathbf{k}), \\
\pm 2\gamma_{\text{ani}}^{\text{new}}(\mathbf{x}) &\equiv \int \frac{d^3k}{(2\pi)^3} e^{i\mathbf{k}\cdot\mathbf{x}} \frac{1}{2} \left[b_K^{(2,0)} \mathcal{G}_{ij}^{(2)}(k) + b_K^{(2,2)} \mathcal{G}_{il}^{(2)}(k) \left(\hat{k}_l \hat{k}_j - \frac{1}{3} \delta_{lj}^K \right) \right. \\
&\quad \left. + b_K^{(4)} \mathcal{G}_{ijkl}^{(4)}(k) \hat{k}_k \hat{k}_l \right] m_i^{\mp}(\hat{x}) m_j^{\mp}(\hat{x}) \bar{\delta}_{\mathbf{m}}(\mathbf{k}),
\end{aligned} \tag{2.17}$$

where $\pm 2\bar{\gamma}$ denotes the isotropy-conserving component, and $\pm 2\gamma_{\text{ani}}^{\text{std}}$ and $\pm 2\gamma_{\text{ani}}^{\text{new}}$ are the isotropy-breaking ones depending on b_K and $(b_K^{(2,0)}, b_K^{(2,2)}, b_K^{(4)})$, respectively. Also about the ellipticity field, there is no distinction between the real and redshift space expressions at linear order of $\bar{\delta}_{\mathbf{m}}$.

2.4 Unified form of the galaxy field

For later convenience, let us express the above three fields (density δ , velocity u and ellipticity $\pm 2\gamma$) using the spin-weighted spherical harmonics. In eqs. (2.9), (2.10) and (2.17), we convert $\mathcal{G}_{i_1 \dots i_L}^{(L)}$ into G_{LM} with eq. (2.7), expand all vectors \hat{k} , \hat{x} , and $\mathbf{m}_{\pm}(\hat{x})$, with the spin-weighted spherical harmonics using eq. (C.1), and simplify the products of the resultant spin-weighted spherical harmonics using the addition theorem (C.4) and (C.5). This computation procedure has been traditionally executed for the CMB polyspectrum computations [46]. The bottom line form is as follow;

$$\begin{aligned}
\lambda X(\mathbf{x}) &= \lambda \bar{X}(\mathbf{x}) + \lambda X_{\text{ani}}^{\text{std}}(\mathbf{x}) + \lambda X_{\text{ani}}^{\text{new}}(\mathbf{x}), \\
\lambda \bar{X}(\mathbf{x}) &\equiv \int \frac{d^3k}{(2\pi)^3} e^{i\mathbf{k}\cdot\mathbf{x}} \sum_j \frac{4\pi c_j^X(k)}{2j+1} \sum_{\mu} Y_{j\mu}(\hat{k})_{-\lambda} Y_{j\mu}^*(\hat{x}) \bar{\delta}_{\mathbf{m}}(\mathbf{k}), \\
\lambda X_{\text{ani}}^{\text{std}}(\mathbf{x}) &\equiv \int \frac{d^3k}{(2\pi)^3} e^{i\mathbf{k}\cdot\mathbf{x}} \sum_j \frac{4\pi c_j^X(k)}{2j+1} \sum_{\mu} Y_{j\mu}(\hat{k})_{-\lambda} Y_{j\mu}^*(\hat{x}) \frac{1}{2} \sum_{L>0} \sum_M G_{LM}(k) Y_{LM}(\hat{k}) \bar{\delta}_{\mathbf{m}}(\mathbf{k}), \\
\lambda X_{\text{ani}}^{\text{new}}(\mathbf{x}) &\equiv \int \frac{d^3k}{(2\pi)^3} e^{i\mathbf{k}\cdot\mathbf{x}} \frac{1}{2} \sum_{Ljj'} e_{Ljj'}^X \sum_{M\mu\mu'} G_{LM}(k) \begin{pmatrix} L & j & j' \\ M & \mu & \mu' \end{pmatrix} Y_{j\mu}^*(\hat{k})_{-\lambda} Y_{j'\mu'}^*(\hat{x}) \bar{\delta}_{\mathbf{m}}(\mathbf{k}),
\end{aligned} \tag{2.18}$$

where $X = \{\delta, u, \gamma\}$ and

$$\begin{aligned}
c_j^\delta(k) &= \left(b_g + \frac{1}{3}f\right) \delta_{j,0}^K - i \frac{\alpha f}{kx} \delta_{j,1}^K + \frac{2}{3}f \delta_{j,2}^K, \\
c_j^u(k) &= i \frac{aHf}{k} \delta_{j,1}^K, \\
c_j^\gamma(k) &= \frac{\sqrt{6}}{3} b_K \delta_{j,2}^K, \\
e_{Ljj'}^\delta &= \sqrt{20\pi} b_g^{(2)} \delta_{L,2}^K \delta_{j,2}^K \delta_{j',0}^K, \\
e_{Ljj'}^u &= 0, \\
e_{Ljj'}^\gamma &= \sqrt{30\pi} b_K^{(2,0)} \delta_{L,2}^K \delta_{j,0}^K \delta_{j',2}^K - \sqrt{\frac{7\pi}{3}} b_K^{(2,2)} \delta_{L,2}^K \delta_{j,2}^K \delta_{j',2}^K + 3\sqrt{\frac{21\pi}{5}} b_K^{(4)} \delta_{L,4}^K \delta_{j,2}^K \delta_{j',2}^K.
\end{aligned} \tag{2.19}$$

The subscript λ in ${}_\lambda X$ represents the spin/helicity dependence of each field; thus, $\lambda = 0$ for $X = \delta, u$, and $\lambda = \pm 2$ for $X = \gamma$. Regarding the spin-0 fields, for notational simplicity, we sometimes omit the subscript 0 in ${}_0 X$ as in eqs. (2.9) and (2.10). For $\lambda = 0$, ${}_\lambda \bar{X}$ in eq. (2.18) recovers the usual Legendre expansion.

3 Efficient computation methodology for general types of the isotropy-breaking galaxy correlations

In this section, we shall build a computation methodology for the galaxy 2PCFs sourced from a general type of the isotropy-breaking matter power spectrum (2.2).

3.1 Isotropy-breaking galaxy correlations

Up to linear order of $G_{L>0,M}$, the 2PCF, $\xi_{\lambda_1 \lambda_2}^{X_1 X_2}(\mathbf{x}_{12}, \hat{x}_1, \hat{x}_2) \equiv \langle {}_{\lambda_1} X_1(\mathbf{x}_1)_{\lambda_2} X_2(\mathbf{x}_2) \rangle$, is computed as

$$\begin{aligned}
\xi_{\lambda_1 \lambda_2}^{X_1 X_2}(\mathbf{x}_{12}, \hat{x}_1, \hat{x}_2) &= \xi_{\lambda_1 \lambda_2}^{X_1 X_2 \text{ std}}(\mathbf{x}_{12}, \hat{x}_1, \hat{x}_2) + \xi_{\lambda_1 \lambda_2}^{X_1 X_2 \text{ new}}(\mathbf{x}_{12}, \hat{x}_1, \hat{x}_2), \\
\xi_{\lambda_1 \lambda_2}^{X_1 X_2 \text{ std}}(\mathbf{x}_{12}, \hat{x}_1, \hat{x}_2) &\equiv \langle {}_{\lambda_1} \bar{X}_1(\mathbf{x}_1)_{\lambda_2} \bar{X}_2(\mathbf{x}_2) \rangle \\
&\quad + \left\langle {}_{\lambda_1} \bar{X}_1(\mathbf{x}_1)_{\lambda_2} X_2^{\text{std}}(\mathbf{x}_2) \right\rangle + \left\langle {}_{\lambda_1} X_1^{\text{std}}(\mathbf{x}_1)_{\lambda_2} \bar{X}_2(\mathbf{x}_2) \right\rangle, \\
\xi_{\lambda_1 \lambda_2}^{X_1 X_2 \text{ new}}(\mathbf{x}_{12}, \hat{x}_1, \hat{x}_2) &\equiv \langle {}_{\lambda_1} \bar{X}_1(\mathbf{x}_1)_{\lambda_2} X_2^{\text{new}}(\mathbf{x}_2) \rangle + \langle {}_{\lambda_1} X_1^{\text{new}}(\mathbf{x}_1)_{\lambda_2} \bar{X}_2(\mathbf{x}_2) \rangle.
\end{aligned} \tag{3.1}$$

Regarding the 2PCFs composed of the density or ellipticity field, $\xi_{\lambda_1 \lambda_2}^{X_1 X_2 \text{ std}}$ and $\xi_{\lambda_1 \lambda_2}^{X_1 X_2 \text{ new}}$ denote the components depending on the standard (b_g, b_K) and new ($b_g^{(2)}, b_K^{(2,0)}, b_K^{(2,2)}, b_K^{(4)}$) bias parameters, respectively. Since $\bar{\delta}_m$ respects the statistical homogeneity, the 2PCF takes the form

$$\xi_{\lambda_1 \lambda_2}^{X_1 X_2}(\mathbf{x}_{12}, \hat{x}_1, \hat{x}_2) = \int \frac{d^3 k}{(2\pi)^3} e^{i\mathbf{k} \cdot \mathbf{x}_{12}} P_{\lambda_1 \lambda_2}^{X_1 X_2}(\mathbf{k}, \hat{x}_1, \hat{x}_2), \tag{3.2}$$

where $\mathbf{x}_{12} \equiv \mathbf{x}_1 - \mathbf{x}_2$. Computing $\xi_{\lambda_1 \lambda_2 \text{std}}^{X_1 X_2}$ and $\xi_{\lambda_1 \lambda_2 \text{new}}^{X_1 X_2}$ by use of eq. (2.18) and the addition theorem (C.4) and (C.5) leads to

$$\begin{aligned}
P_{\lambda_1 \lambda_2}^{X_1 X_2}(\mathbf{k}, \hat{x}_1, \hat{x}_2) &= P_{\lambda_1 \lambda_2 \text{std}}^{X_1 X_2}(\mathbf{k}, \hat{x}_1, \hat{x}_2) + P_{\lambda_1 \lambda_2 \text{new}}^{X_1 X_2}(\mathbf{k}, \hat{x}_1, \hat{x}_2), \\
P_{\lambda_1 \lambda_2 \text{std}}^{X_1 X_2}(\mathbf{k}, \hat{x}_1, \hat{x}_2) &\equiv \bar{P}_m(k) \sum_{LM} G_{LM}(k) Y_{LM}(\hat{k}) \sum_{J j_1 j_2} \frac{(4\pi)^2 (-1)^{j_2} h_{J j_1 j_2}^{0 0 0}}{(2j_1 + 1)(2j_2 + 1)} c_{j_1}^{X_1}(k) c_{j_2}^{X_2}(k) \\
&\quad \times \sum_{\mu \mu_1 \mu_2} \begin{pmatrix} J & j_1 & j_2 \\ \mu & \mu_1 & \mu_2 \end{pmatrix} Y_{J\mu}^*(\hat{k})_{-\lambda_1} Y_{j_1 \mu_1}^*(\hat{x}_1)_{-\lambda_2} Y_{j_2 \mu_2}^*(\hat{x}_2), \\
P_{\lambda_1 \lambda_2 \text{new}}^{X_1 X_2}(\mathbf{k}, \hat{x}_1, \hat{x}_2) &\equiv \frac{1}{2} \bar{P}_m(k) \sum_{L j_1 j_2 j'} \sum_{M \mu_1 \mu_2 \mu'} G_{LM}(k) Y_{j_1 \mu_1}(\hat{k}) (-1)^{j_2} Y_{j_2 \mu_2}(\hat{k}) \\
&\quad \times \left[\frac{4\pi c_{j_1}^{X_1}(k)}{2j_1 + 1} e_{L j_2 j'}^{X_2} \begin{pmatrix} L & j_2 & j' \\ M & -\mu_2 & \mu' \end{pmatrix} (-1)^{\mu_2 - \lambda_1} Y_{j_1 \mu_1}^*(\hat{x}_1)_{-\lambda_2} Y_{j' \mu'}^*(\hat{x}_2) \right. \\
&\quad \left. + \frac{4\pi c_{j_2}^{X_2}(k)}{2j_2 + 1} e_{L j_1 j'}^{X_1} \begin{pmatrix} L & j_1 & j' \\ M & -\mu_1 & \mu' \end{pmatrix} (-1)^{\mu_1 - \lambda_2} Y_{j_2 \mu_2}^*(\hat{x}_2)_{-\lambda_1} Y_{j' \mu'}^*(\hat{x}_1) \right], \tag{3.3}
\end{aligned}$$

where $h_{l_1 l_2 l_3}^{s_1 s_2 s_3} \equiv \sqrt{\frac{(2l_1+1)(2l_2+1)(2l_3+1)}{4\pi}} \begin{pmatrix} l_1 & l_2 & l_3 \\ s_1 & s_2 & s_3 \end{pmatrix}$. We note that $P_{\lambda_1 \lambda_2}^{X_1 X_2}(\mathbf{k}, \hat{x}_1, \hat{x}_2)$ is not the Fourier counterpart of $\xi_{\lambda_1 \lambda_2}^{X_1 X_2}(\mathbf{x}_{12}, \hat{x}_1, \hat{x}_2)$.

The relation between $\xi_{\lambda_1 \lambda_2}^{X_1 X_2}$ and the angular correlation function defined on the celestial sphere $\langle \lambda_1 a_{\ell_1 m_1}^{X_1} \lambda_2 a_{\ell_2 m_2}^{X_2} \rangle$ is summarized in appendix B.

3.2 Spin-weighted tripolar spherical harmonic decomposition approach for the exact analysis

As confirmed in refs. [12, 38, 40, 41], the PolypoSH decomposition approach is an efficient and fast way to compute the isotropy-breaking 2PCFs of the spin-0 fields such as the density δ and the velocity u . We here generalize it to deal with the higher-spin fields as the ellipticity $\pm 2\gamma$. Our generalized formulae recover the 2PCFs obtained in ref. [37] at the isotropy-conserving limit.

Let us start from the computation without assuming the PP approximation. Since the 2PCF (3.2) is characterized by \hat{x}_{12} , \hat{x}_1 and \hat{x}_2 , let us introduce a basis function of these three directions, i.e., the spin-weighted TripoSH:

$$\begin{aligned}
\lambda_1 \lambda_2 \mathcal{X}_{\ell \ell_1 \ell_2 \ell'}^{LM}(\hat{x}_{12}, \hat{x}_1, \hat{x}_2) &\equiv \{Y_\ell(\hat{x}_{12}) \otimes \{\lambda_1 Y_{\ell_1}(\hat{x}_1) \otimes \lambda_2 Y_{\ell_2}(\hat{x}_2)\}_{\ell'}\}_{LM} \\
&= \sum_{m m_1 m_2 m'} \mathcal{C}_{\ell m \ell' m'}^{LM} \mathcal{C}_{\ell_1 m_1 \ell_2 m_2}^{\ell' m'} Y_{\ell m}(\hat{x}_{12})_{\lambda_1} Y_{\ell_1 m_1}(\hat{x}_1)_{\lambda_2} Y_{\ell_2 m_2}(\hat{x}_2), \tag{3.4}
\end{aligned}$$

and perform the following decomposition:

$$\xi_{\lambda_1 \lambda_2}^{X_1 X_2}(\mathbf{x}_{12}, \hat{x}_1, \hat{x}_2) = \sum_{\ell \ell_1 \ell_2 \ell' LM} \lambda_1 \lambda_2 \Xi_{\ell \ell_1 \ell_2 \ell'}^{LM X_1 X_2}(x_{12})_{\lambda_1 \lambda_2} \mathcal{X}_{\ell \ell_1 \ell_2 \ell'}^{LM}(\hat{x}_{12}, \hat{x}_1, \hat{x}_2), \tag{3.5}$$

where $\mathcal{C}_{\ell_1 m_1 \ell_2 m_2}^{\ell m_3} \equiv (-1)^{l_1 - l_2 + m_3} \sqrt{2l_3 + 1} \begin{pmatrix} l_1 & l_2 & l_3 \\ m_1 & m_2 & -m_3 \end{pmatrix}$ is the Clebsch-Gordan coefficient.

To obtain the TripoSH coefficient ${}_{\lambda_1\lambda_2}\Xi_{\ell\ell_1\ell_2\ell'}^{LMX_1X_2}$, we also decompose $P_{\lambda_1\lambda_2}^{X_1X_2}$ as

$$P_{\lambda_1\lambda_2}^{X_1X_2}(\mathbf{k}, \hat{x}_1, \hat{x}_2) = \sum_{\ell\ell_1\ell_2\ell'LM} {}_{\lambda_1\lambda_2}\Pi_{\ell\ell_1\ell_2\ell'}^{LMX_1X_2}(k) {}_{\lambda_1\lambda_2}\mathcal{X}_{\ell\ell_1\ell_2\ell'}^{LM}(\hat{k}, \hat{x}_1, \hat{x}_2). \quad (3.6)$$

Substituting this into eq. (3.2), performing the \hat{k} integral by use of eq. (C.4), and comparing the resultant $\xi_{\lambda_1\lambda_2}^{X_1X_2}$ with eq. (3.5), we derive the Hankel transformation rule:

$${}_{\lambda_1\lambda_2}\Xi_{\ell\ell_1\ell_2\ell'}^{LMX_1X_2}(x_{12}) = i^\ell \int_0^\infty \frac{k^2 dk}{2\pi^2} j_\ell(kx_{12}) {}_{\lambda_1\lambda_2}\Pi_{\ell\ell_1\ell_2\ell'}^{LMX_1X_2}(k). \quad (3.7)$$

This is computed after obtaining ${}_{\lambda_1\lambda_2}\Pi_{\ell\ell_1\ell_2\ell'}^{LMX_1X_2}$ by use of

$${}_{\lambda_1\lambda_2}\Pi_{\ell\ell_1\ell_2\ell'}^{LMX_1X_2}(k) = \int d^2\hat{k} \int d^2\hat{x}_1 \int d^2\hat{x}_2 P_{\lambda_1\lambda_2}^{X_1X_2}(\mathbf{k}, \hat{x}_1, \hat{x}_2) {}_{\lambda_1\lambda_2}\mathcal{X}_{\ell\ell_1\ell_2\ell'}^{LM*}(\hat{k}, \hat{x}_1, \hat{x}_2). \quad (3.8)$$

Let us estimate ${}_{\lambda_1\lambda_2}\Pi_{\ell\ell_1\ell_2\ell'}^{LMX_1X_2}$ from eq. (3.3). Performing the spherical harmonic integrals and simplifying the resultant Wigner symbols by use of eqs. (C.4) and (C.5), we obtain

$$\begin{aligned} {}_{\lambda_1\lambda_2}\Pi_{\ell\ell_1\ell_2\ell'}^{LMX_1X_2}(k) &= {}_{\lambda_1\lambda_2}\Pi_{\ell\ell_1\ell_2\ell' \text{ std}}^{LMX_1X_2}(k) + {}_{\lambda_1\lambda_2}\Pi_{\ell\ell_1\ell_2\ell' \text{ new}}^{LMX_1X_2}(k), \\ {}_{\lambda_1\lambda_2}\Pi_{\ell\ell_1\ell_2\ell' \text{ std}}^{LMX_1X_2}(k) &\equiv \bar{P}_m(k) G_{LM}(k) \frac{(4\pi)^2 (-1)^{\lambda_1+\lambda_2+\ell_1+L} h_{\ell_1\ell_2\ell'}^{000} h_{\ell\ell'L}^{000}}{(2\ell_1+1)(2\ell_2+1)\sqrt{2\ell'+1}\sqrt{2L+1}} c_{\ell_1}^{X_1}(k) c_{\ell_2}^{X_2}(k), \\ {}_{\lambda_1\lambda_2}\Pi_{\ell\ell_1\ell_2\ell' \text{ new}}^{LMX_1X_2}(k) &\equiv \frac{1}{2} \bar{P}_m(k) G_{LM}(k) (-1)^{\lambda_1+\lambda_2} \sqrt{\frac{2\ell'+1}{2L+1}} \sum_j \\ &\quad \times \left[\frac{4\pi c_{\ell_1}^{X_1}(k)}{2\ell_1+1} e_{Lj\ell_2}^{X_2} h_{\ell_1j\ell}^{000} \begin{Bmatrix} \ell & \ell' & L \\ \ell_2 & j & \ell_1 \end{Bmatrix} (-1)^{\ell+\ell_1+\ell_2} \right. \\ &\quad \left. + \frac{4\pi c_{\ell_2}^{X_2}(k)}{2\ell_2+1} e_{Lj\ell_1}^{X_1} h_{\ell_2j\ell}^{000} \begin{Bmatrix} \ell & \ell' & L \\ \ell_1 & j & \ell_2 \end{Bmatrix} (-1)^{\ell'} \right]. \end{aligned} \quad (3.9)$$

The number of nonvanishing multipoles is restricted by the selection rules in c_j^X , $e_{Ljj'}^X$ [see eq. (2.19)] and $h_{\ell_1\ell_2\ell_3}^{s_1s_2s_3}$. From eq. (3.9), it is apparent that nonvanishing G_{LM} is linearly reflected on ${}_{\lambda_1\lambda_2}\Pi_{\ell\ell_1\ell_2\ell'}^{LMX_1X_2}$. Note that ${}_{\lambda_1\lambda_2}\Pi_{\ell\ell_1\ell_2\ell'}^{00X_1X_2}$ or ${}_{\lambda_1\lambda_2}\Xi_{\ell\ell_1\ell_2\ell'}^{00X_1X_2}$ completely recovers the TripoSH coefficient computed from the isotropy-conserving matter power spectrum in ref. [37] because of $G_{00} = \sqrt{4\pi}$, $h_{\ell\ell'0}^{000} = (-1)^\ell \sqrt{\frac{2\ell+1}{4\pi}} \delta_{\ell\ell'}^K$ and ${}_{\lambda_1\lambda_2}\Pi_{\ell\ell_1\ell_2\ell' \text{ new}}^{00X_1X_2} = 0$.

Figure 1 depicts all nonvanishing $L = 2$ TripoSH coefficients of the $\delta\gamma$, $u\gamma$ and $\gamma\gamma$ correlations as a function of x_{12} . Here we assume $G_{LM} \propto k^0$, so that G_{LM} can be singled out in the TripoSH coefficient as ${}_{\lambda_1\lambda_2}\Xi_{\ell\ell_1\ell_2\ell'}^{LMX_1X_2} = \frac{G_{LM}}{\sqrt{4\pi}} {}_{\lambda_1\lambda_2}\Xi_{\ell\ell_1\ell_2\ell'}^{LX_1X_2}$. This figure rather shows the reduced coefficient ${}_{\lambda_1\lambda_2}\Xi_{\ell\ell_1\ell_2\ell'}^{2X_1X_2}$. At each multipole, the baryon acoustic oscillation (BAO) bump at $x_{12} \simeq 100h^{-1}$ Mpc is confirmed. It is also apparent that the redshift-space distortion (RSD) effect induces higher multipoles in the $\delta\gamma$ correlation, making the difference in shape between the real and redshift space 2PCFs as seen in section 4 and appendix A.

The results in figure 1 are utilized for computing the 2PCFs of the g_* model in section 4.

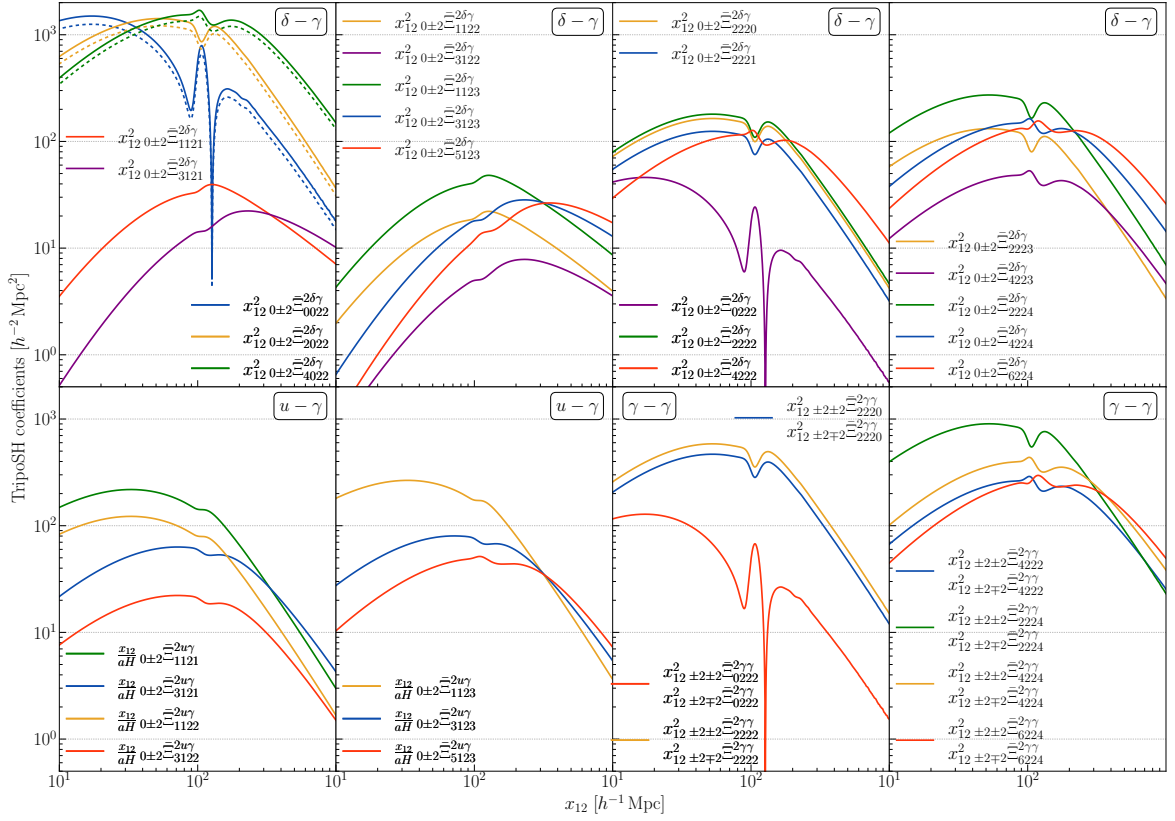


Figure 1. Absolute values of all reduced TripoSH coefficients for $L = 2$: $0\pm 2\Xi_{\ell\ell_1\ell_2\ell'}^{2\delta\gamma}$ (top four panels), $0\pm 2\Xi_{\ell\ell_1\ell_2\ell'}^{2u\gamma}$ (bottom left two panels) and $\pm 2\pm 2\Xi_{\ell\ell_1\ell_2\ell'}^{2\gamma\gamma} = \pm 2\mp 2\Xi_{\ell\ell_1\ell_2\ell'}^{2\gamma\gamma}$ (bottom right two panels) as a function of x_{12} for $z_1 = z_2 = 0.3$ and $b_g = b_g^{(2)} = b_K = b_K^{(2,0)} = b_K^{(2,2)} = 1$. Solid and dashed lines discriminate between the results in the redshift and real spaces, respectively. Note that the reduced TripoSH coefficient $\lambda_1\lambda_2\Xi_{\ell\ell_1\ell_2\ell'}^{LX_1X_2}$ is defined as the original TripoSH one $\lambda_1\lambda_2\Xi_{\ell\ell_1\ell_2\ell'}^{LMX_1X_2}$ divided by $G_{LM}/\sqrt{4\pi}$ when $G_{LM} \propto k^0$ and therefore independent of G_{LM} .

3.3 Spin-weighted bipolar spherical harmonic decomposition approach for the plane-parallel-limit analysis

In the following, we reduce the above expression to that in the PP limit. In this limit, the 2PCF is characterized by \hat{x}_{12} and \hat{x}_p that is a LOS direction chosen as satisfying $\hat{x}_p \simeq \hat{x}_1 \simeq \hat{x}_2$; therefore, the decomposition formula reduces to

$$\begin{aligned} \xi_{\lambda_1\lambda_2\text{PP}}^{X_1X_2}(\mathbf{x}_{12}, \hat{x}_p) &\equiv \xi_{\lambda_1\lambda_2}^{X_1X_2}(\mathbf{x}_{12}, \hat{x}_p, \hat{x}_p) \\ &= \sum_{\ell\ell'LM} \lambda_1\lambda_2 \xi_{\ell\ell'}^{LMX_1X_2}(x_{12})_{\lambda_1+\lambda_2} X_{\ell\ell'}^{LM}(\hat{x}_{12}, \hat{x}_p), \end{aligned} \quad (3.10)$$

where the spin-weighted Biposh basis is defined as

$$\begin{aligned} \lambda' X_{\ell\ell'}^{LM}(\hat{x}_{12}, \hat{x}_p) &\equiv \{Y_\ell(\hat{x}_{12}) \otimes \lambda' Y_{\ell'}(\hat{x}_p)\}_{LM} \\ &= \sum_{mm'} c_{\ell m \ell' m'}^{LM} Y_{\ell m}(\hat{x}_{12}) \lambda' Y_{\ell' m'}(\hat{x}_p). \end{aligned} \quad (3.11)$$

In a similar manner to the TripoSH decomposition, we perform the Fourier-space pre-decomposition:

$$\begin{aligned} P_{\lambda_1\lambda_2\text{PP}}^{X_1X_2}(\mathbf{k}, \hat{x}_p) &\equiv P_{\lambda_1\lambda_2}^{X_1X_2}(\mathbf{k}, \hat{x}_p, \hat{x}_p) \\ &= \sum_{\ell\ell'LM} \lambda_1\lambda_2 \pi_{\ell\ell'}^{LMX_1X_2}(k)_{\lambda_1+\lambda_2} X_{\ell\ell'}^{LM}(\hat{k}, \hat{x}_p). \end{aligned} \quad (3.12)$$

With this, eqs. (3.2), (3.10) and the identities in appendix C, we derive the Hankel transformation formula:

$$\lambda_1\lambda_2 \xi_{\ell\ell'}^{LMX_1X_2}(x_{12}) = i^\ell \int_0^\infty \frac{k^2 dk}{2\pi^2} j_\ell(kx_{12})_{\lambda_1\lambda_2} \pi_{\ell\ell'}^{LMX_1X_2}(k), \quad (3.13)$$

where

$$\lambda_1\lambda_2 \pi_{\ell\ell'}^{LMX_1X_2}(k) = \int d^2\hat{k} \int d^2\hat{x}_p P_{\lambda_1\lambda_2\text{PP}}^{X_1X_2}(\mathbf{k}, \hat{x}_p)_{\lambda_1+\lambda_2} X_{\ell\ell'}^{LM*}(\hat{k}, \hat{x}_p). \quad (3.14)$$

Because of the relation between the TripoSH and BipoSH bases:

$$\lambda_1\lambda_2 \mathcal{X}_{\ell\ell_1\ell_2\ell'}^{LM}(\hat{x}_{12}, \hat{x}_p, \hat{x}_p) = (-1)^{\ell_1-\ell_2+\lambda_1+\lambda_2} \frac{h_{\ell_1}^{-\lambda_1} h_{\ell_2}^{-\lambda_2} h_{\ell'}^{\lambda_1+\lambda_2}}{\sqrt{2\ell'+1}} \lambda_1\lambda_2 X_{\ell\ell'}^{LM}(\hat{x}_{12}, \hat{x}_p), \quad (3.15)$$

the BipoSH coefficients can directly be inverted from the TripoSH ones as

$$\begin{aligned} \lambda_1\lambda_2 \xi_{\ell\ell'}^{LMX_1X_2}(x_{12}) &= \sum_{\ell_1\ell_2} (-1)^{\ell_1-\ell_2+\lambda_1+\lambda_2} \frac{h_{\ell_1}^{-\lambda_1} h_{\ell_2}^{-\lambda_2} h_{\ell'}^{\lambda_1+\lambda_2}}{\sqrt{2\ell'+1}} \lambda_1\lambda_2 \Xi_{\ell\ell_1\ell_2\ell'}^{LMX_1X_2}(x_{12}), \\ \lambda_1\lambda_2 \pi_{\ell\ell'}^{LMX_1X_2}(k) &= \sum_{\ell_1\ell_2} (-1)^{\ell_1-\ell_2+\lambda_1+\lambda_2} \frac{h_{\ell_1}^{-\lambda_1} h_{\ell_2}^{-\lambda_2} h_{\ell'}^{\lambda_1+\lambda_2}}{\sqrt{2\ell'+1}} \lambda_1\lambda_2 \Pi_{\ell\ell_1\ell_2\ell'}^{LMX_1X_2}(k). \end{aligned} \quad (3.16)$$

Plugging eq. (3.3) into eq. (3.14) and simplifying the integrals, or more simply, computing eq. (3.16) with eq. (3.9), we obtain

$$\begin{aligned} \lambda_1\lambda_2 \pi_{\ell\ell'}^{LMX_1X_2}(k) &= \lambda_1\lambda_2 \pi_{\ell\ell'\text{std}}^{LMX_1X_2}(k) + \lambda_1\lambda_2 \pi_{\ell\ell'\text{new}}^{LMX_1X_2}(k), \\ \lambda_1\lambda_2 \pi_{\ell\ell'\text{std}}^{LMX_1X_2}(k) &\equiv \bar{P}_m(k) G_{LM}(k) \sum_{\ell_1\ell_2} \frac{(4\pi)^2 (-1)^{\ell_2+L} h_{\ell_1}^{-\lambda_1} h_{\ell_2}^{-\lambda_2} h_{\ell'}^{\lambda_1+\lambda_2} h_{\ell_1\ell_2\ell'}^0 h_{\ell\ell'L}^{000}}{(2\ell_1+1)(2\ell_2+1)(2\ell'+1)\sqrt{2L+1}} c_{\ell_1}^{X_1}(k) c_{\ell_2}^{X_2}(k), \\ \lambda_1\lambda_2 \pi_{\ell\ell'\text{new}}^{LMX_1X_2}(k) &\equiv \frac{1}{2} \bar{P}_m(k) G_{LM}(k) \sum_{\ell_1\ell_2} \frac{h_{\ell_1}^{-\lambda_1} h_{\ell_2}^{-\lambda_2} h_{\ell'}^{\lambda_1+\lambda_2}}{\sqrt{2L+1}} \sum_j \\ &\times \left[\frac{4\pi c_{\ell_1}^{X_1}(k)}{2\ell_1+1} e_{Lj\ell_2}^{X_2} h_{\ell_1j\ell}^{000} \begin{Bmatrix} \ell & \ell' & L \\ \ell_2 & j & \ell_1 \end{Bmatrix} (-1)^\ell \right. \\ &\left. + \frac{4\pi c_{\ell_2}^{X_2}(k)}{2\ell_2+1} e_{Lj\ell_1}^{X_1} h_{\ell_2j\ell}^{000} \begin{Bmatrix} \ell & \ell' & L \\ \ell_1 & j & \ell_2 \end{Bmatrix} (-1)^{\ell_1+\ell_2+\ell'} \right]. \end{aligned} \quad (3.17)$$

The isotropy-conserving matter power spectrum induces only $\lambda_1\lambda_2 \pi_{\ell\ell'}^{00X_1X_2}$ or $\lambda_1\lambda_2 \xi_{\ell\ell'}^{00X_1X_2}$. The 2PCFs computed from these fully recover the results in ref. [43].³

³The 2PCFs computed in ref. [43], ξ_{g+} , ξ_{v+} and ξ_{\pm} , are related to ours according to $\xi_{g+} = \xi_{0+2}^{\delta\gamma} + \xi_{0-2}^{\delta\gamma}$, $\xi_{v+} = \xi_{0+2}^{u\gamma} + \xi_{0-2}^{u\gamma}$ and $\xi_{\pm} = 2(\xi_{+2\mp 2}^{\gamma\gamma} + \xi_{-2\pm 2}^{\gamma\gamma})$.

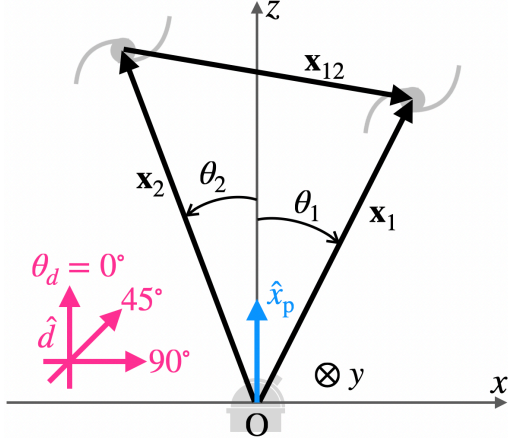


Figure 2. Coordinate system adopted in the computation of the 2PCFs using the exact form $\xi_{\lambda_1\lambda_2}^{X_1X_2}(\mathbf{x}_{12}, \hat{x}_1, \hat{x}_2)$ and the PP approximation $\xi_{\lambda_1\lambda_2\text{PP}}^{X_1X_2}(\mathbf{x}_{12}, \hat{x}_p)$.

4 Correlations of the ellipticity field in the g_* model

Now we move to the numerical computation of the 2PCFs for a concrete scenario where the matter power spectrum includes a scale-invariant isotropy-breaking term whose magnitude is parametrized by g_* , reading

$$\begin{aligned} P_m(\mathbf{k}) &= \bar{P}_m(k) \left[1 + g_* \left\{ (\hat{k} \cdot \hat{d})^2 - \frac{1}{3} \right\} \right] \\ &= \bar{P}_m(k) \left[\mathcal{L}_0(\hat{k} \cdot \hat{d}) + \frac{2}{3} g_* \mathcal{L}_2(\hat{k} \cdot \hat{d}) \right], \end{aligned} \quad (4.1)$$

where \hat{d} denotes some global preferred direction, and $\mathcal{L}_\ell(x)$ is the Legendre polynomial. With eq. (C.1), one can find the form of G_{LM} in eq. (2.2) and $\mathcal{G}_{i_1 \dots i_L}^{(L)}$ in eq. (2.5) as

$$\begin{aligned} G_{LM} &= \sqrt{4\pi} \delta_{L,0}^K \delta_{M,0}^K + \frac{8\pi}{15} g_* Y_{2M}^*(\hat{d}) \delta_{L,2}^K, \\ \mathcal{G}_{i_1 \dots i_L}^{(L)} &= g_* \left(\hat{d}_{i_1} \hat{d}_{i_2} - \frac{1}{3} \delta_{i_1 i_2}^K \right) \delta_{L,2}^K. \end{aligned} \quad (4.2)$$

As confirmed in the previous section, the former (G_{00}) and latter (G_{2M}) terms make nonvanishing TripoSH coefficients ${}_{\lambda_1\lambda_2} \Xi_{\ell\ell_1\ell_2\ell'}^{00X_1X_2}$ and ${}_{\lambda_1\lambda_2} \Xi_{\ell\ell_1\ell_2\ell'}^{2MX_1X_2}$, respectively. For late convenience, let us notationally differentiate the 2PCF to two terms as

$$\xi_{\lambda_1\lambda_2}^{X_1X_2} = {}^{(0)}\xi_{\lambda_1\lambda_2}^{X_1X_2} + g_* {}^{(2)}\xi_{\lambda_1\lambda_2}^{X_1X_2}. \quad (4.3)$$

The former and latter terms correspond to the isotropy-conserving and isotropy-breaking parts, respectively.

The matter power spectrum (2.2) for $G_{L>0,M} \neq 0$ can be generated by the existence of some anisotropic source. If there are (spin-1) vector fields which couple to inflaton or non-inflaton scalar ones in the inflationary era, nonvanishing g_* or G_{2M} arises as well as G_{00} (e.g., refs. [47–54]). In more general, spin- s fields produce nonzero G_{00} , G_{2M} , G_{4M} , \dots , $G_{2(s-1),M}$

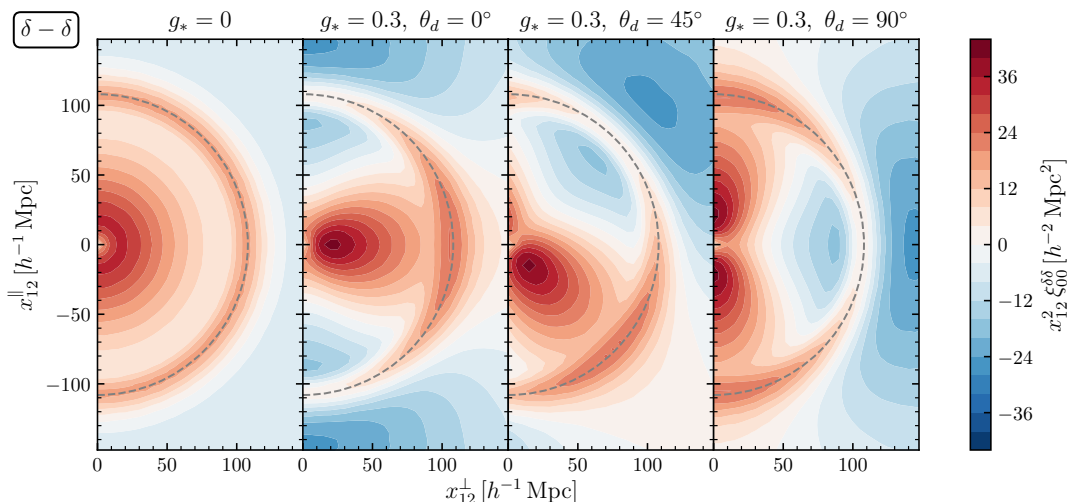


Figure 3. Intensity distributions of the real-space $\delta\bar{\delta}$ correlation in the PP limit on the $(x_{12}^{\perp}, x_{12}^{\parallel})$ plane for $z_1 = z_2 = 0.3$ and $b_g = b_g^{(2)} = 1$. The leftmost and the other three right panels show the results of the g_* model for $g_* = 0$ and 0.3 , respectively (we consider such a large g_* to highlight the isotropy-breaking signatures although it is disfavored by observations). For the latter, three different \hat{d} : $\theta_d = 0^\circ, 45^\circ$ and 90° are considered. The region for $x_{12}^{\perp} \geq 0$ is only shown, while one can reconstruct the region for $x_{12}^{\perp} < 0$ as these 2PCFs are symmetric or antisymmetric with respect to the origin. For reference, the BAO scale, $x_{12} \simeq 100h^{-1}$ Mpc, is displayed with the dashed grey circles.

and $G_{2s,M}$ [39, 55]. Other kinds of sources, e.g., two-form fields [56], an inflating solid or elastic medium [57, 58], fossil gravitational waves [59–62] and large scale tides beyond the survey region [40, 63–66] also induce nonvanishing $G_{L>0,M}$. The spectral shape of the induced G_{LM} relies on the choice of, e.g., the coupling function and the potential of the fields. In the following 2PCF computations, let us focus on the simplest case where g_* becomes constant in wavenumber. By the recent analysis with the CMB [8] and galaxy density fields [12], $|g_*| > \mathcal{O}(10^{-2})$ is disfavored.

To make our discussion simpler, we shall work on the coordinate system where the three direction vectors \hat{x}_{12} , \hat{x}_1 and \hat{x}_2 are on the xz plane and parametrized as $\hat{x}_{12} = (\sin\theta_{12}, 0, \cos\theta_{12})$, $\hat{x}_1 = (\sin\theta_1, 0, \cos\theta_1)$ and $\hat{x}_2 = (-\sin\theta_2, 0, \cos\theta_2)$ (here, the polar angles are fixed as $\phi_{12} = \phi_1 = 0$ and $\phi_2 = \pi$). In the PP limit; namely, $\theta_1 \rightarrow 0$ and $\theta_2 \rightarrow 0$, the two different LOS directions \hat{x}_1 and \hat{x}_2 can be identified with the z -axis positive direction, so that $\hat{x}_p = (0, 0, 1)$. In the following, we examine how the 2PCFs are distorted depending on the preferred direction $\hat{d} = (\sin\theta_d \cos\phi_d, \sin\theta_d \sin\phi_d, \cos\theta_d)$ by considering three different cases: $\theta_d = 0^\circ, 45^\circ$ and 90° with $\phi_d = 0$, equivalently, $\hat{d} = (0, 0, 1)$, $(\frac{1}{\sqrt{2}}, 0, \frac{1}{\sqrt{2}})$ and $(1, 0, 0)$. For $\theta_d = 0^\circ$ and 90° , $\hat{d} = \hat{x}_p$ and $\hat{d} \perp \hat{x}_p$ hold, respectively. Even investigating $90^\circ \leq \theta_d \leq 180^\circ$, the symmetric results are obtained. Moreover, the distortion shapes depend weakly on the y -axis component of \hat{d} , so that we do not pick up any other \hat{d} . The coordinate system and settings mentioned above are visually summarized in figure 2.

We shall first assess the shape change of the 2PCFs depending on \hat{d} based on the PP-limit results. For this purpose, we analyze $\xi_{\lambda_1\lambda_2}^{X_1X_2}(\mathbf{x}_{12}, \hat{x}_p)$ as a function of x_{12}^{\perp} and x_{12}^{\parallel} , the components of \mathbf{x}_{12} perpendicular and parallel to the LOS direction \hat{x}_p . In the computation,

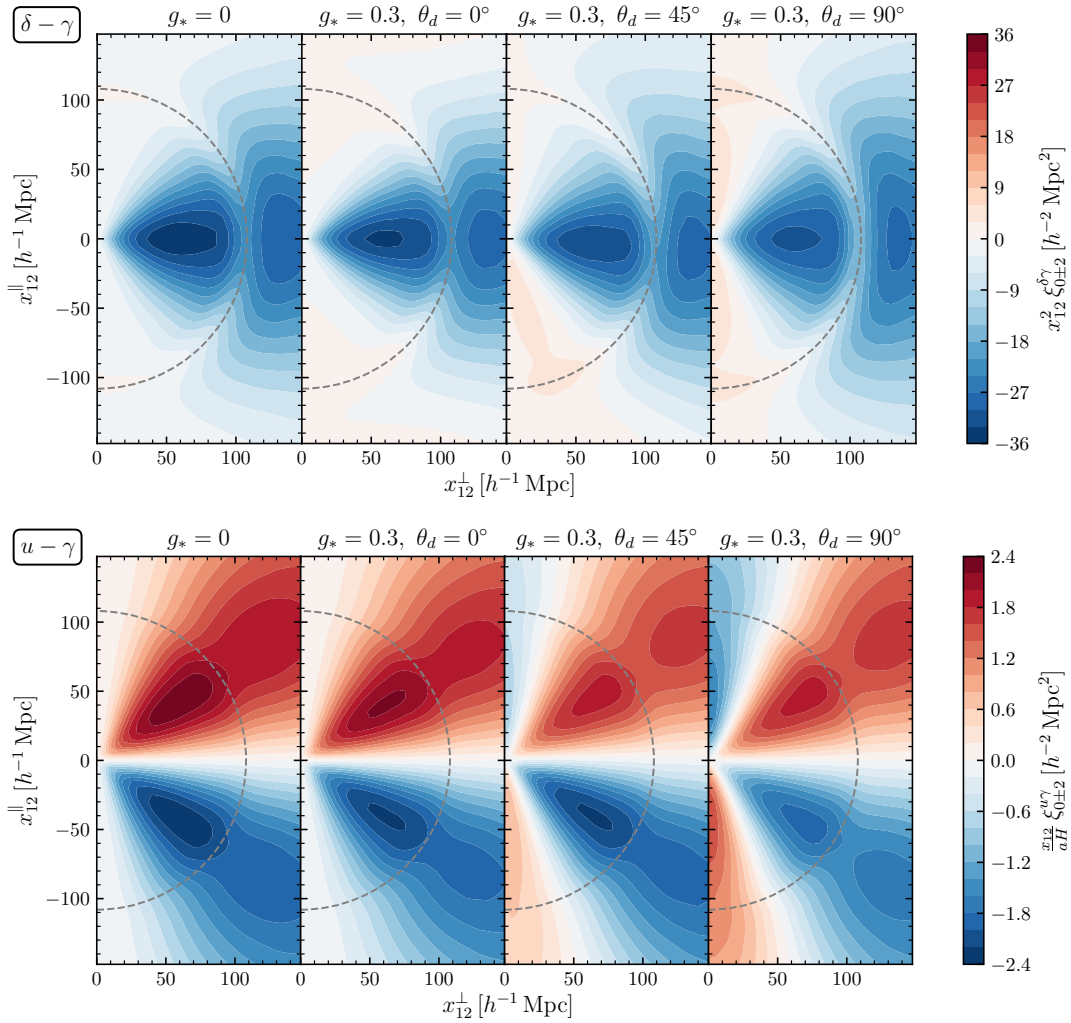


Figure 4. Same as figure 3, except for the $\delta\gamma$ correlation in the redshift space and the $u\gamma$ correlation when $b_g = b_g^{(2)} = b_K = b_K^{(2,0)} = b_K^{(2,2)} = 1$.

we set $\mathbf{x}_{12} = (x_{12}^\perp, 0, x_{12}^\parallel)$ and thus adopt $\theta_{12} = \arccos(\hat{x}_{12} \cdot \hat{x}_p) = \arccos(x_{12}^\parallel/x_{12})$ and $x_{12} = \sqrt{(x_{12}^\perp)^2 + (x_{12}^\parallel)^2}$. Figures 3, 4, 5 and 7 depict the results for several g_* and θ_d .

Here, let us begin with the assessment of the $\delta\delta$ correlations in the real space as the isotropy-breaking signatures are most clearly apparent there. From figure 3, one can easily find that nonzero g_* distorts the 2PCF depending on θ_d . For $\theta_d = 0^\circ$, since $\hat{x}_p = \hat{d}$, the 2PCF is distorted along the x_{12}^\perp axis. This looks similar to the RSD effect in the redshift-space $\delta\delta$ correlation (top leftmost panel in figure 7). On the other hand, for $\theta_d = 90^\circ$ and 45° , the distortions seem to appear in a direction along the x_{12}^\parallel axis and the diagonal line, respectively. Such a feature could be a distinctive indicator for testing the cosmic isotropy. For the other types of the 2PCFs described in figures 4, 5 and 7, the isotropy-breaking signatures due to nonzero g_* are sometimes degenerate with the isotropy-conserving ones when $g_* = 0$, and the above trend is then slightly perceptible.

We further go through the 2PCF beyond the PP limit by use of the TripoSH decomposition technique. For numerical computations of $\xi_{\lambda_1\lambda_2}^{X_1X_2}(\mathbf{x}_{12}, \hat{x}_1, \hat{x}_2)$, we impose $\hat{x}_{12} = (1, 0, 0)$

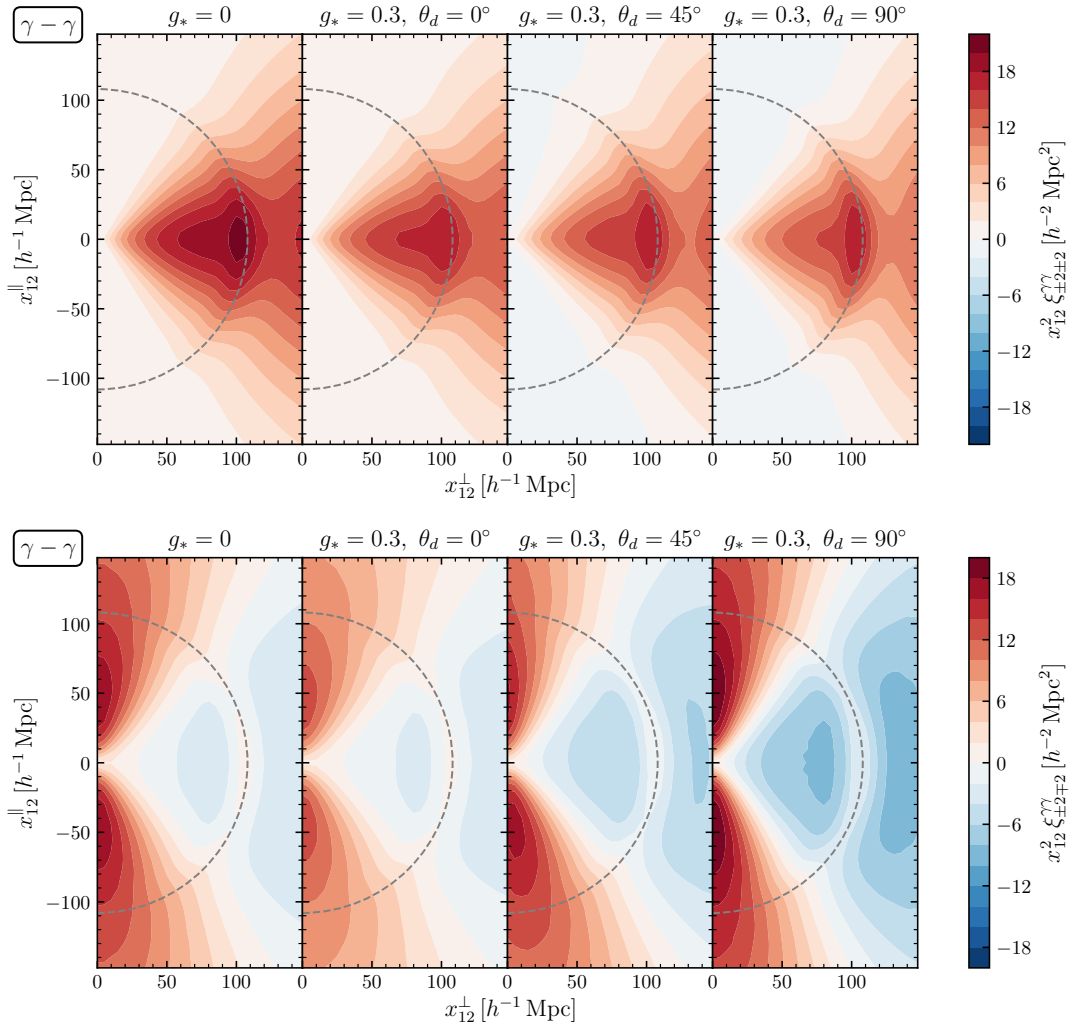


Figure 5. Same as figure 3, except for the $\gamma\gamma$ correlation when $b_K = b_K^{(2,0)} = b_K^{(2,2)} = 1$.

(i.e., $\theta_{12} = 90^\circ$) and $\theta_1 = \theta_2$ and define the opening angle between \hat{x}_1 and \hat{x}_2 as $\Theta \equiv \theta_1 + \theta_2 = 2\theta_1 = 2\theta_2$. Due to these conditions, a triangle formed by \mathbf{x}_{12} , \mathbf{x}_1 and \mathbf{x}_2 becomes isosceles.

The results of the $\delta\gamma$, $u\gamma$ and $\gamma\gamma$ correlations including nonzero g_* at several x_{12} or Θ are summarized in figure 6. One can confirm from this that the distortion level of the 2PCF for a certain g_* changes depending on θ_d . It is enhanced as θ_d increases for the $\delta\gamma$ or $\gamma\gamma$ case, while maximized at $\theta_d \sim 45^\circ$ for the $u\gamma$ one (see the top panels). The latter feature is confirmed also from the δu correlations (see figure 8).

From figure 6, one can also study how accurate the PP approximation is. The ratios between the exact and approximate results of the isotropy-breaking parts of the 2PCFs given in eq. (4.3), ${}^{(2)}\xi_{\lambda_1\lambda_2}^{X_1X_2} / {}^{(2)}\xi_{\lambda_1\lambda_2}^{X_1X_2}_{\text{PP}}$, are plotted in the bottom panels. Basically, as Θ increases, this ratio departs from unity, meaning that the error of the PP approximation becomes larger. In the $\gamma\gamma$ case, for any θ_d , the PP approximation works, at least, up to $\Theta \sim 10^\circ$ because the error is within 10%. Similar but better results are obtained in the $\delta\delta$ and uu cases (see figure 8). In contrast, the $\delta\gamma$ case is sensitive to θ_d , and if $\theta_d = 45^\circ$, the accuracy drops drastically and the error exceeds 10% already at $\Theta \sim 5^\circ$. For the $u\gamma$ case, even worse, the

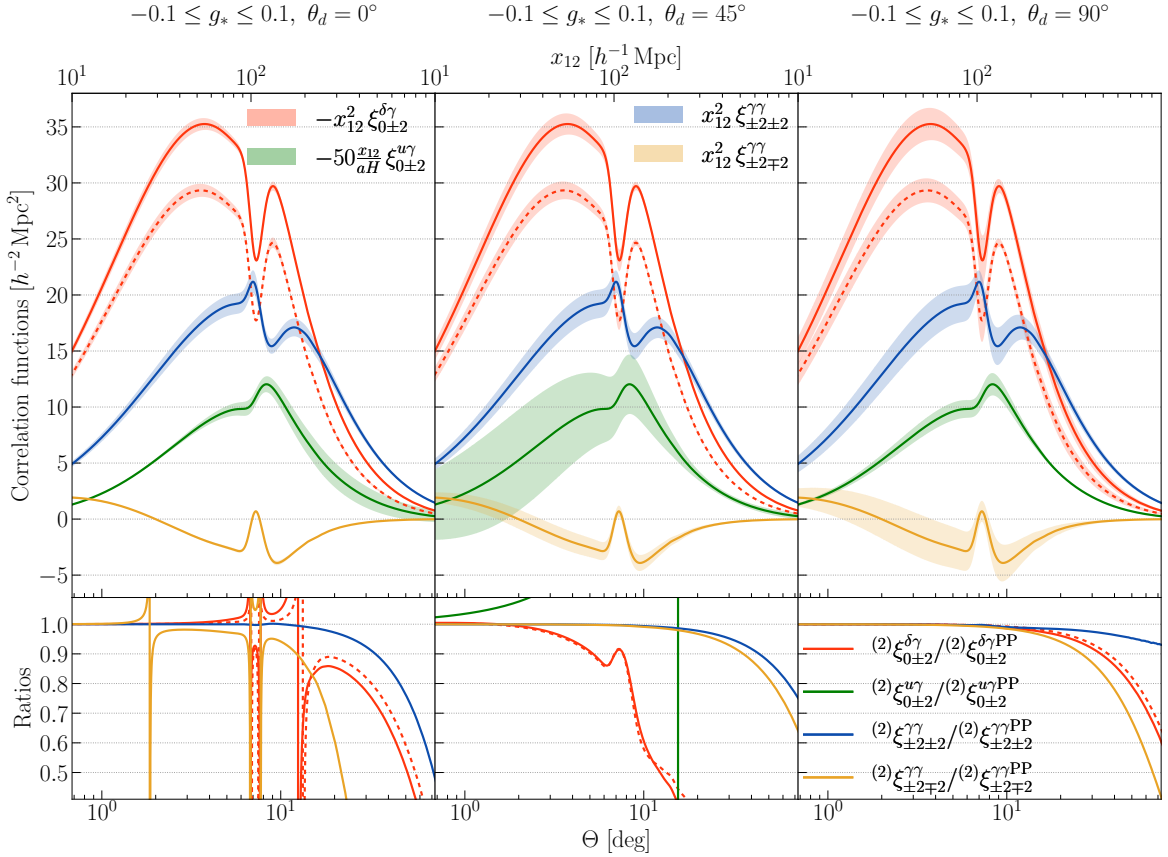


Figure 6. Absolute values of the 2PCFs $\xi_{\lambda_1 \lambda_2}^{X_1 X_2}$ of the g_* model for $-0.1 \leq g_* \leq 0.1$ (top panels) and ratios between the exact and PP-limit results of the isotropy-breaking parts $(2)\xi_{\lambda_1 \lambda_2}^{X_1 X_2}$ (bottom panels) for the $\delta\gamma$, $u\gamma$ and $\gamma\gamma$ cases as a function of Θ or x_{12} when $z_1 = z_2 = 0.3$ and $b_g = b_g^{(2)} = b_K = b_K^{(2,0)} = b_K^{(2,2)} = 1$. Here, three different \hat{d} : $\theta_d = 0^\circ$ (left panels), 45° (center panels) and 90° (right panels) are considered. In the top panels, the 2PCFs move under a range of g_* and are thus expressed with the finite-width lines (the central lines correspond to the results for $g_* = 0$). Solid and dashed lines discriminate between the results in the redshift and real spaces, respectively. Note that all the results in the bottom panels are independent of g_* . In the bottom panels, some spiky features appear or some lines entirely disappear as $(2)\xi_{\lambda_1 \lambda_2 \text{PP}}^{X_1 X_2}$ sometimes vanish.

PP approximation is totally spoiled. These indicate the importance of the analysis without the PP approximation for an accurate estimation of g_* . We note that, regarding the isotropy-conserving part $(0)\xi_{\lambda_1 \lambda_2}^{X_1 X_2}$, for the $\delta\gamma$ and $\gamma\gamma$ cases, the PP approximation works under $\Theta \lesssim 30^\circ$ as shown in ref. [37].

5 Conclusions

In this paper, we have studied the impacts of the cosmic isotropy breaking on the 2PCFs of the galaxy intrinsic alignment or equivalently the spin-2 galaxy ellipticity field for the first time. To achieve this, we first have developed a formalism for general types of the isotropy-breaking 2PCFs and an efficient computation methodology of them by generalizing

the standard PolypoSH decomposition to the spin-weighted version. This is applicable to not only the analysis with the PP approximation but also the exact analysis. The previous spin-0 version of our computation methodology has already been implemented also for measuring galaxy clustering [12]. Since the new spin-weighted one is comparably speedy and efficient, it could also work in the data analysis with the ellipticity field.

As a concrete demonstration, we have analyzed the 2PCFs in a well-known g_* model according to this methodology. It has been confirmed that some isotropy-breaking distortions appear in the 2PCFs, and their shapes rely on a preferred direction causing the isotropy violation \hat{d} . Such a feature could be a distinctive indicator for testing the cosmic isotropy.⁴ Comparing between the exact and the PP-limit results, we have quantified the error of the PP approximation as a function of an opening angle between the LOS directions towards target galaxies Θ . For the ellipticity auto correlation, the error does not exceed 10% at $\Theta \lesssim 10^\circ$ for any \hat{d} . For the density-ellipticity and velocity-ellipticity cross correlations, the error is enhanced for specific \hat{d} , and the validity of the PP approximation is no longer guaranteed even at $\Theta = \mathcal{O}(1^\circ)$. This suggests the importance of the analysis beyond the PP approximation for an accurate isotropy test.

In the practical analysis, we have focused on the g_* model, in which the matter power spectrum is given by eq. (4.1), predicting nonzero TripoSH monopole and quadrupole, $\lambda_{1\lambda_2} \Xi_{\ell\ell_1\ell_2\ell'}^{00X_1X_2}$ and $\lambda_{1\lambda_2} \Xi_{\ell\ell_1\ell_2\ell'}^{2MX_1X_2}$. On the other hand, in other models that could yield nonzero higher multipoles $\lambda_{1\lambda_2} \Xi_{\ell\ell_1\ell_2\ell'}^{L>2, MX_1X_2}$ as mentioned in section 4, the 2PCFs would be distorted in a different fashion. Moreover, including contributions due to not only the matter distribution (scalar mode) but also the vorticity (vector mode) and the gravitational wave (tensor mode) [62, 67, 68] might yield other unique shapes in the 2PCFs. These could also be dealt with by our spin-weighted PolypoSH decomposition methodology owing to its high versatility, and should be studied in future works.

Our results have been obtained on the basis of the linear theory and hence might increase ambiguity at smaller scales. It should be checked with N-body simulations and the higher-order perturbation theory as done in ref. [69].

Acknowledgments

M. S. is supported by JSPS KAKENHI Grant Nos. JP19K14718, JP20H05859 and JP23K03390. T. O. acknowledges support from the Ministry of Science and Technology of Taiwan under Grant Nos. MOST 110-2112-M-001-045- and MOST 111-2112-M-001-061- and the Career Development Award, Academia Sinica (AS-CDA-108-M02) for the period of 2019 to 2023. K. A. is supported by JSPS Overseas Research Fellowships. M. S. and K. A. also acknowledge the Center for Computational Astrophysics, National Astronomical Observatory of Japan, for providing the computing resources of the Cray XC50.

A Correlations of the density and velocity fields in the g_* model

Here we summarize the same results as in section 4 but for the $\delta\delta$, δu and uu cases.

Figure 7 describes the intensity distributions of the $\delta\delta$, δu and uu correlations in the PP limit on the $(x_{12}^\perp, x_{12}^\parallel)$ domain for nonzero g_* and several θ_d . One can observe the distortions

⁴There remain some parameter degeneracies between the intrinsic isotropy-breaking parameters G_{LM} and the galaxy bias parameters in the 2PCFs (see sections 2 and 3); hence, a careful treatment is necessary in the practical data analysis.

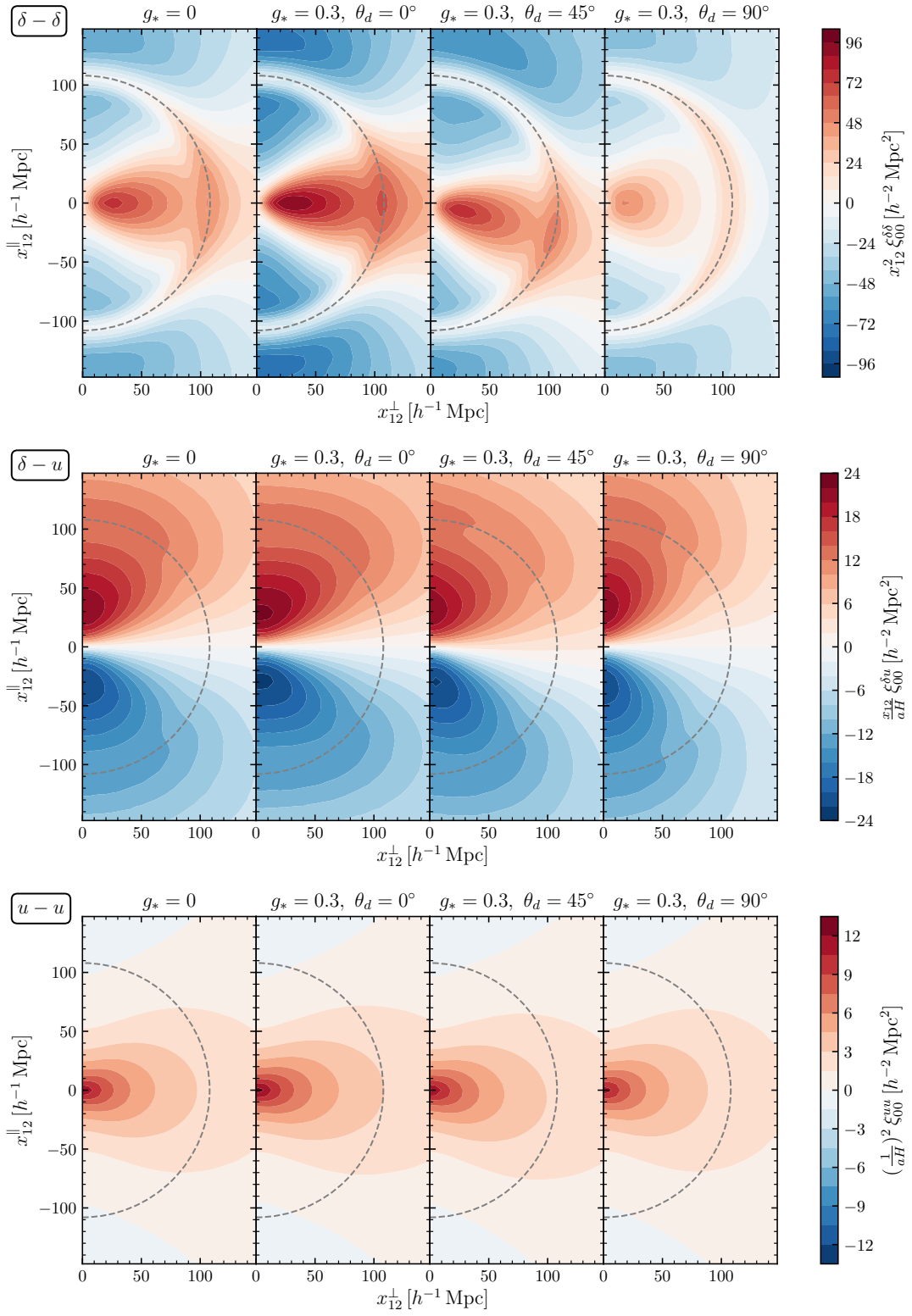


Figure 7. Same as figure 3, except for the $\delta\delta$ and δu correlations in the redshift space and the uu one.

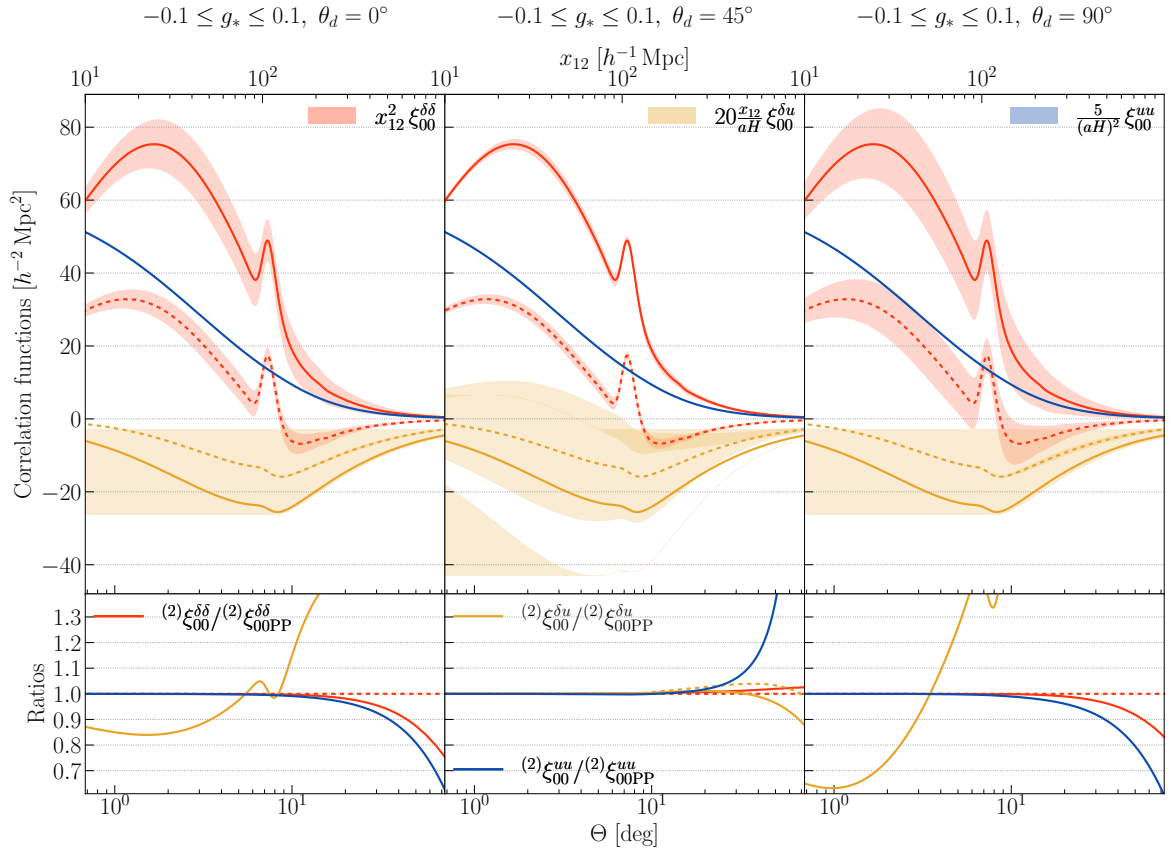


Figure 8. Same as figure 6, except for the $\delta\delta$, δu and uu cases.

by nonzero g_* along the x_{12}^\perp axis, the diagonal line and the x_{12}^\parallel axis for $\theta_d = 0^\circ$, 45° and 90° , respectively, similarly to the $\delta\gamma$, $u\gamma$ and $\gamma\gamma$ cases.

Figure 8 depicts the $\delta\delta$, δu and uu correlations and the ratios between the exact and PP-limit results of their isotropy-breaking parts as a function of x_{12} or Θ for nonzero g_* and several θ_d . The top panels indicate that the distortion level in the uu , δu or $\delta\delta$ correlation for a certain g_* varies depending on θ_d , and is maximized for $\theta_d \sim 0^\circ$, 45° or 90° . The bottom panels show that the PP approximation works independently of θ_d when $\Theta \lesssim 30^\circ$ for the $\delta\delta$ and uu cases, while its validity is not guaranteed even when $\Theta \sim 1^\circ$ for the δu case with $\theta_d = 0^\circ$ and 90° .

B Angular correlation functions

We here summarize the relation between the configuration-space correlations discussed in the main text and the angular correlations.

The spin- $|\lambda|$ field ${}_\lambda X$ can be generally expanded with the spin-weighted spherical harmonics as

$${}_\lambda X(\mathbf{x}) = \sum_{\ell m} {}_\lambda a_{\ell m}^X {}_\lambda Y_{\ell m}(\hat{x}). \quad (\text{B.1})$$

Computing the inverse formula:

$$\lambda a_{\ell m}^X = \int d^2 \hat{x} \lambda X(\mathbf{x}) \lambda Y_{\ell m}^*(\hat{x}), \quad (\text{B.2})$$

with eqs. (2.18), (C.4) and (C.5), we obtain

$$\begin{aligned} \lambda a_{\ell m}^X &= \lambda \bar{a}_{\ell m}^X + \lambda a_{\ell m}^{X \text{ std}} + \lambda a_{\ell m}^{X \text{ new}}, \\ \lambda \bar{a}_{\ell m}^X &\equiv 4\pi i^\ell \int \frac{d^3 k}{(2\pi)^3} \bar{\delta}_m(\mathbf{k}) Y_{\ell m}^*(\hat{k}) \lambda \mathcal{T}_\ell^X(k), \\ \lambda a_{\ell m}^{X \text{ std}} &\equiv 4\pi i^\ell \int \frac{d^3 k}{(2\pi)^3} \bar{\delta}_m(\mathbf{k}) \sum_{\ell' m'} Y_{\ell' m'}^*(\hat{k}) \frac{1}{2} \sum_{L>0} \sum_M G_{LM}(k) (-1)^m \begin{pmatrix} \ell & \ell' & L \\ -m & m' & M \end{pmatrix} h_{\ell \ell' L}^{000} \lambda \mathcal{T}_\ell^X(k), \\ \lambda a_{\ell m}^{X \text{ new}} &\equiv 4\pi i^\ell \int \frac{d^3 k}{(2\pi)^3} \bar{\delta}_m(\mathbf{k}) \sum_{\ell' m'} Y_{\ell' m'}^*(\hat{k}) \frac{1}{2} \sum_{LM} G_{LM}(k) (-1)^m \begin{pmatrix} \ell & \ell' & L \\ -m & m' & M \end{pmatrix} \lambda \mathcal{S}_{\ell \ell' L}^X(k), \end{aligned} \quad (\text{B.3})$$

where

$$\begin{aligned} \lambda \mathcal{T}_\ell^X(k) &\equiv \sum_{jj'} \frac{4\pi i^{j-\ell} h_{jj'\ell}^{000} h_{jj'\ell}^{0\lambda-\lambda}}{(2\ell+1)(2j'+1)} c_{j'}^X(k) j_j(kx), \\ \lambda \mathcal{S}_{\ell \ell' L}^X(k) &\equiv \sum_{jj'J} i^{J-\ell} (-1)^J e_{Ljj'}^X h_{Jj'\ell}^{0\lambda-\lambda} h_{Jj\ell'}^{000} \begin{Bmatrix} \ell & \ell' & L \\ j & j' & J \end{Bmatrix} j_J(kx), \end{aligned} \quad (\text{B.4})$$

and c_j^X and $e_{Ljj'}^X$ are defined in eq. (2.19).

Up to linear order of $G_{L>0,M}$, the angular correlation is given as

$$\begin{aligned} \left\langle \lambda_1 a_{\ell_1 m_1}^{X_1} \lambda_2 a_{\ell_2 m_2}^{X_2} \right\rangle &= \left\langle \lambda_1 \bar{a}_{\ell_1 m_1}^{X_1} \lambda_2 \bar{a}_{\ell_2 m_2}^{X_2} \right\rangle + \left\langle \lambda_1 \bar{a}_{\ell_1 m_1}^{X_1} \lambda_2 a_{\ell_2 m_2}^{X_2 \text{ std}} \right\rangle + \left\langle \lambda_1 a_{\ell_1 m_1}^{X_1 \text{ std}} \lambda_2 \bar{a}_{\ell_2 m_2}^{X_2} \right\rangle \\ &+ \left\langle \lambda_1 \bar{a}_{\ell_1 m_1}^{X_1} \lambda_2 a_{\ell_2 m_2}^{X_2 \text{ new}} \right\rangle + \left\langle \lambda_1 a_{\ell_1 m_1}^{X_1 \text{ new}} \lambda_2 \bar{a}_{\ell_2 m_2}^{X_2} \right\rangle. \end{aligned} \quad (\text{B.5})$$

Computing this with eqs. (B.3) and (C.4) leads to

$$\left\langle \lambda_1 a_{\ell_1 m_1}^{X_1} \lambda_2 a_{\ell_2 m_2}^{X_2} \right\rangle = i^{\ell_1 - \ell_2} (-1)^{m_1 + m_2} \sum_{LM} \begin{pmatrix} \ell_1 & \ell_2 & L \\ -m_1 & -m_2 & M \end{pmatrix} \lambda_1 \lambda_2 C_{\ell_1 \ell_2}^{LM X_1 X_2}, \quad (\text{B.6})$$

where

$$\begin{aligned} \lambda_1 \lambda_2 C_{\ell_1 \ell_2}^{LM X_1 X_2} &= \lambda_1 \lambda_2 C_{\ell_1 \ell_2}^{LM X_1 X_2 \text{ std}} + \lambda_1 \lambda_2 C_{\ell_1 \ell_2}^{LM X_1 X_2 \text{ new}}, \\ \lambda_1 \lambda_2 C_{\ell_1 \ell_2}^{LM X_1 X_2 \text{ std}} &\equiv \frac{2}{\pi} \int_0^\infty k^2 dk \bar{P}_m(k) G_{LM}(k) \lambda_1 \mathcal{T}_{\ell_1}^{X_1}(k) \lambda_2 \mathcal{T}_{\ell_2}^{X_2}(k) h_{\ell_1 \ell_2 L}^{000}, \\ \lambda_1 \lambda_2 C_{\ell_1 \ell_2}^{LM X_1 X_2 \text{ new}} &\equiv \frac{2}{\pi} \int_0^\infty k^2 dk \bar{P}_m(k) G_{LM}(k) \frac{1}{2} \left[\lambda_1 \mathcal{T}_{\ell_1}^{X_1}(k) \lambda_2 \mathcal{S}_{\ell_2 \ell_1 L}^{X_2}(k) + \lambda_2 \mathcal{T}_{\ell_2}^{X_2}(k) \lambda_1 \mathcal{S}_{\ell_1 \ell_2 L}^{X_1}(k) \right]. \end{aligned} \quad (\text{B.7})$$

Nonzero $G_{L>0,M}$ generated from the isotropy-violating matter power spectrum induce nonzero off-diagonal modes $\ell_1 \neq \ell_2$. The 2PCF $\xi_{\lambda_1 \lambda_2}^{X_1 X_2}$ is related to $\lambda_1 \lambda_2 C_{\ell_1 \ell_2}^{LM X_1 X_2}$ as

$$\begin{aligned} \xi_{\lambda_1 \lambda_2}^{X_1 X_2}(\mathbf{x}_{12}, \hat{x}_1, \hat{x}_2) &= \sum_{\ell_1 m_1 \ell_2 m_2} i^{\ell_1 - \ell_2} (-1)^{m_1 + m_2} \sum_{LM} \begin{pmatrix} \ell_1 & \ell_2 & L \\ -m_1 & -m_2 & M \end{pmatrix} \\ &\times \lambda_1 \lambda_2 C_{\ell_1 \ell_2}^{LM X_1 X_2} \lambda_1 Y_{\ell_1 m_1}(\hat{x}_1) \lambda_2 Y_{\ell_2 m_2}(\hat{x}_2). \end{aligned} \quad (\text{B.8})$$

The spin-2 ellipticity field ${}_{\pm 2}\gamma$ can be converted into the spin-0 E/B-mode one, whose harmonic coefficient is given by⁵

$$\begin{aligned} {}_0a_{\ell m}^E &\equiv -\frac{1}{2} \left({}_{+2}a_{\ell m}^\gamma + {}_{-2}a_{\ell m}^\gamma \right), \\ {}_0a_{\ell m}^B &\equiv -\frac{1}{2i} \left({}_{+2}a_{\ell m}^\gamma - {}_{-2}a_{\ell m}^\gamma \right). \end{aligned} \quad (\text{B.9})$$

The angular correlation composed of ${}_0a_{\ell m}^{E/B}$ also takes the form (B.6); and because ${}_{-\lambda}\mathcal{T}_\ell^X = {}_\lambda\mathcal{T}_\ell^X$ and ${}_{-\lambda}\mathcal{S}_{\ell\ell'L}^X = (-1)^{\ell+\ell'} {}_\lambda\mathcal{S}_{\ell\ell'L}^X$, the following relations hold

$$\begin{aligned} {}_{00}C_{\ell_1\ell_2}^{LM,\delta/u,E} &= -{}_{0+2}C_{\ell_1\ell_2\text{std}}^{LM,\delta/u,\gamma} - \frac{1 + (-1)^{\ell_1+\ell_2}}{2} {}_{0+2}C_{\ell_1\ell_2\text{new}}^{LM,\delta/u,\gamma}, \\ {}_{00}C_{\ell_1\ell_2}^{LM,\delta/u,B} &= -\frac{1 - (-1)^{\ell_1+\ell_2}}{2i} {}_{0+2}C_{\ell_1\ell_2\text{new}}^{LM,\delta/u,\gamma}, \\ {}_{00}C_{\ell_1\ell_2}^{LMEE} &= {}_{+2+2}C_{\ell_1\ell_2\text{std}}^{LM\gamma\gamma} + \frac{1 + (-1)^{\ell_1+\ell_2}}{4} \left({}_{+2+2}C_{\ell_1\ell_2\text{new}}^{LM\gamma\gamma} + {}_{+2-2}C_{\ell_1\ell_2\text{new}}^{LM\gamma\gamma} \right), \\ {}_{00}C_{\ell_1\ell_2}^{LMEB} &= \frac{1 - (-1)^{\ell_1+\ell_2}}{4i} \left({}_{+2+2}C_{\ell_1\ell_2\text{new}}^{LM\gamma\gamma} - {}_{+2-2}C_{\ell_1\ell_2\text{new}}^{LM\gamma\gamma} \right), \\ {}_{00}C_{\ell_1\ell_2}^{LMBB} &= -\frac{1 + (-1)^{\ell_1+\ell_2}}{4} \left({}_{+2+2}C_{\ell_1\ell_2\text{new}}^{LM\gamma\gamma} - {}_{+2-2}C_{\ell_1\ell_2\text{new}}^{LM\gamma\gamma} \right). \end{aligned} \quad (\text{B.10})$$

These indicate that $\langle {}_0a_{\ell_1 m_1}^{\delta/u/E} {}_0a_{\ell_2 m_2}^B \rangle$ and $\langle {}_0a_{\ell_1 m_1}^B {}_0a_{\ell_2 m_2}^B \rangle$ do not vanish when $\ell_1 + \ell_2 = \text{odd}$ and even, respectively.

C Useful mathematical identities

The spherical harmonic decompositions: [46]

$$\begin{aligned} \mathcal{L}_l(\hat{k} \cdot \hat{x}) &= \frac{4\pi}{2l+1} \sum_m Y_{lm}(\hat{k}) Y_{lm}^*(\hat{x}), \\ e^{i\mathbf{k} \cdot \mathbf{x}} &= \sum_{lm} 4\pi i^l j_l(kx) Y_{lm}(\hat{k}) Y_{lm}^*(\hat{x}), \\ \hat{k} &= \sum_m \boldsymbol{\alpha}^m Y_{1m}(\hat{k}), \\ \mathbf{m}_\pm(\hat{x}) &= \pm \sum_m \boldsymbol{\alpha}^{m \mp 1} Y_{1m}(\hat{x}), \end{aligned} \quad (\text{C.1})$$

where a m -dependent vector $\boldsymbol{\alpha}^m$, given by

$$\boldsymbol{\alpha}^m \equiv \sqrt{\frac{2\pi}{3}} \begin{pmatrix} -m(\delta_{m,1}^K + \delta_{m,-1}^K) \\ i(\delta_{m,1}^K + \delta_{m,-1}^K) \\ \sqrt{2}\delta_{m,0}^K \end{pmatrix}, \quad (\text{C.2})$$

satisfies $(\boldsymbol{\alpha}^m)^* = (-1)^m \boldsymbol{\alpha}^{-m}$ and

$$\begin{aligned} \boldsymbol{\alpha}^{m_1} \cdot \boldsymbol{\alpha}^{m_2} &= \frac{4\pi}{3} (-1)^{m_1} \delta_{m_1, -m_2}^K, \\ \sum_m \alpha_i^m \alpha_j^{m*} &= \frac{4\pi}{3} \delta_{ij}^K. \end{aligned} \quad (\text{C.3})$$

⁵See refs. [16, 68] for another convention that is different by sign from ours.

The addition theorem and the orthonormality of the spin-weighted spherical harmonics:

$$\begin{aligned}
s_1 Y_{l_1 m_1}(\hat{n}) s_2 Y_{l_2 m_2}(\hat{n}) &= \sum_{s_3 l_3 m_3} s_3 Y_{l_3 m_3}^*(\hat{n}) h_{l_1 l_2 l_3}^{-s_1 - s_2 - s_3} \begin{pmatrix} l_1 & l_2 & l_3 \\ m_1 & m_2 & m_3 \end{pmatrix}, \\
\int d^2 \hat{n} s Y_{l_1 m_1}(\hat{n}) s Y_{l_2 m_2}^*(\hat{n}) &= \delta_{l_1, l_2}^K \delta_{m_1, m_2}^K.
\end{aligned} \tag{C.4}$$

The addition theorem of the Wigner symbols:

$$\begin{aligned}
\frac{\delta_{l_3, l'_3}^K \delta_{m_3, m'_3}^K}{2l_3 + 1} &= \sum_{m_1 m_2} \begin{pmatrix} l_1 & l_2 & l_3 \\ m_1 & m_2 & m_3 \end{pmatrix} \begin{pmatrix} l_1 & l_2 & l'_3 \\ m_1 & m_2 & m'_3 \end{pmatrix}, \\
\begin{pmatrix} l_1 & l_2 & l_3 \\ m_1 & m_2 & m_3 \end{pmatrix} \begin{Bmatrix} l_1 & l_2 & l_3 \\ l_4 & l_5 & l_6 \end{Bmatrix} &= \sum_{m_4 m_5 m_6} (-1)^{\sum_{i=4}^6 (l_i - m_i)} \begin{pmatrix} l_5 & l_1 & l_6 \\ m_5 & -m_1 & -m_6 \end{pmatrix} \\
&\quad \times \begin{pmatrix} l_6 & l_2 & l_4 \\ m_6 & -m_2 & -m_4 \end{pmatrix} \begin{pmatrix} l_4 & l_3 & l_5 \\ m_4 & -m_3 & -m_5 \end{pmatrix}, \\
\begin{pmatrix} l_1 & l_2 & l_3 \\ m_1 & m_2 & m_3 \end{pmatrix} \begin{Bmatrix} l_1 & l_2 & l_3 \\ l_4 & l_5 & l_6 \\ l_7 & l_8 & l_9 \end{Bmatrix} &= \sum_{\substack{m_4 m_5 m_6 \\ m_7 m_8 m_9}} \begin{pmatrix} l_4 & l_5 & l_6 \\ m_4 & m_5 & m_6 \end{pmatrix} \begin{pmatrix} l_7 & l_8 & l_9 \\ m_7 & m_8 & m_9 \end{pmatrix} \begin{pmatrix} l_4 & l_7 & l_1 \\ m_4 & m_7 & m_1 \end{pmatrix} \\
&\quad \times \begin{pmatrix} l_5 & l_8 & l_2 \\ m_5 & m_8 & m_2 \end{pmatrix} \begin{pmatrix} l_6 & l_9 & l_3 \\ m_6 & m_9 & m_3 \end{pmatrix}.
\end{aligned} \tag{C.5}$$

The angular integral over a product of unit vectors: [70, 71]

$$\begin{aligned}
\int d^2 \hat{k} \prod_{r=1}^{2n} \hat{k}_{i_r} &= \frac{4\pi}{(2n+1)!!} \left[\delta_{i_1 i_2}^K \delta_{i_3 i_4}^K \cdots \delta_{i_{2n-1} i_{2n}}^K + \{(2n-1)!! - 1 \text{ perms}\} \right], \\
\int d^2 \hat{k} \prod_{r=1}^{2n-1} \hat{k}_{i_r} &= 0,
\end{aligned} \tag{C.6}$$

where $n \in \mathbb{N}$.

References

- [1] E. Dimastrogiovanni, N. Bartolo, S. Matarrese and A. Riotto, *Non-Gaussianity and Statistical Anisotropy from Vector Field Populated Inflationary Models*, *Adv. Astron.* **2010** (2010) 752670, [1001.4049].
- [2] J. Soda, *Statistical Anisotropy from Anisotropic Inflation*, *Class. Quant. Grav.* **29** (2012) 083001, [1201.6434].
- [3] A. Maleknejad, M. Sheikh-Jabbari and J. Soda, *Gauge Fields and Inflation*, *Phys.Rept.* **528** (2013) 161–261, [1212.2921].
- [4] J. Beltran Jimenez and A. L. Maroto, *A cosmic vector for dark energy*, *Phys. Rev. D* **78** (2008) 063005, [0801.1486].
- [5] T. Hambye, *Hidden vector dark matter*, *JHEP* **01** (2009) 028, [0811.0172].
- [6] P. W. Graham, J. Mardon and S. Rajendran, *Vector Dark Matter from Inflationary Fluctuations*, *Phys. Rev. D* **93** (2016) 103520, [1504.02102].

- [7] M. Bastero-Gil, J. Santiago, L. Ubaldi and R. Vega-Morales, *Vector dark matter production at the end of inflation*, *JCAP* **04** (2019) 015, [[1810.07208](#)].
- [8] PLANCK collaboration, Y. Akrami et al., *Planck 2018 results. X. Constraints on inflation*, *Astron. Astrophys.* **641** (2020) A10, [[1807.06211](#)].
- [9] PLANCK collaboration, Y. Akrami et al., *Planck 2018 results. VII. Isotropy and Statistics of the CMB*, *Astron. Astrophys.* **641** (2020) A7, [[1906.02552](#)].
- [10] PLANCK collaboration, Y. Akrami et al., *Planck 2018 results. IX. Constraints on primordial non-Gaussianity*, *Astron. Astrophys.* **641** (2020) A9, [[1905.05697](#)].
- [11] A. R. Pullen and C. M. Hirata, *Non-detection of a statistically anisotropic power spectrum in large-scale structure*, *JCAP* **05** (2010) 027, [[1003.0673](#)].
- [12] N. S. Sugiyama, M. Shiraishi and T. Okumura, *Limits on statistical anisotropy from BOSS DR12 galaxies using bipolar spherical harmonics*, *Mon. Not. Roy. Astron. Soc.* **473** (2018) 2737–2752, [[1704.02868](#)].
- [13] N. E. Chisari and C. Dvorkin, *Cosmological Information in the Intrinsic Alignments of Luminous Red Galaxies*, *JCAP* **12** (2013) 029, [[1308.5972](#)].
- [14] F. Schmidt, N. E. Chisari and C. Dvorkin, *Imprint of inflation on galaxy shape correlations*, *JCAP* **10** (2015) 032, [[1506.02671](#)].
- [15] N. E. Chisari, C. Dvorkin, F. Schmidt and D. Spergel, *Multitracing Anisotropic Non-Gaussianity with Galaxy Shapes*, *Phys. Rev. D* **94** (2016) 123507, [[1607.05232](#)].
- [16] K. Kogai, T. Matsubara, A. J. Nishizawa and Y. Urakawa, *Intrinsic galaxy alignment from angular dependent primordial non-Gaussianity*, *JCAP* **08** (2018) 014, [[1804.06284](#)].
- [17] T. Okumura, A. Taruya and T. Nishimichi, *Intrinsic alignment statistics of density and velocity fields at large scales: Formulation, modeling and baryon acoustic oscillation features*, *Phys. Rev. D* **100** (2019) 103507, [[1907.00750](#)].
- [18] A. Taruya and T. Okumura, *Improving geometric and dynamical constraints on cosmology with intrinsic alignments of galaxies*, *Astrophys. J. Lett.* **891** (2020) L42, [[2001.05962](#)].
- [19] K. Kogai, K. Akitsu, F. Schmidt and Y. Urakawa, *Galaxy imaging surveys as spin-sensitive detector for cosmological colliders*, *JCAP* **03** (2021) 060, [[2009.05517](#)].
- [20] K. Akitsu, T. Kurita, T. Nishimichi, M. Takada and S. Tanaka, *Imprint of anisotropic primordial non-Gaussianity on halo intrinsic alignments in simulations*, *Phys. Rev. D* **103** (2021) 083508, [[2007.03670](#)].
- [21] T. Okumura and A. Taruya, *Tightening geometric and dynamical constraints on dark energy and gravity: Galaxy clustering, intrinsic alignment, and kinetic Sunyaev-Zel’dovich effect*, *Phys. Rev. D* **106** (2022) 043523, [[2110.11127](#)].
- [22] S. Saga, T. Okumura, A. Taruya and T. Inoue, *Relativistic distortions in galaxy density–ellipticity correlations: gravitational redshift and peculiar velocity effects*, *Mon. Not. Roy. Astron. Soc.* **518** (2023) 4976–4990, [[2207.03454](#)].
- [23] T. Okumura and A. Taruya, *First Constraints on Growth Rate from Redshift-space Ellipticity Correlations of SDSS Galaxies at $0.16 < z < 0.70$* , *Astrophys. J. Lett.* **945** (2023) L30, [[2301.06273](#)].
- [24] T. Kurita and M. Takada, *Constraints on anisotropic primordial non-Gaussianity from intrinsic alignments of SDSS-III BOSS galaxies*, [2302.02925](#).
- [25] Z. Vlah, N. E. Chisari and F. Schmidt, *An EFT description of galaxy intrinsic alignments*, *JCAP* **01** (2020) 025, [[1910.08085](#)].
- [26] Z. Vlah, N. E. Chisari and F. Schmidt, *Galaxy shape statistics in the effective field theory*, *JCAP* **05** (2021) 061, [[2012.04114](#)].

- [27] T. Matsubara, *The integrated perturbation theory for cosmological tensor fields I: Basic formulation*, [2210.10435](#).
- [28] T. Matsubara, *The integrated perturbation theory for cosmological tensor fields II: Loop corrections*, [2210.11085](#).
- [29] A. S. Szalay, T. Matsubara and S. D. Landy, *Redshift space distortions of the correlation function in wide angle galaxy surveys*, *Astrophys. J. Lett.* **498** (1998) L1, [[astro-ph/9712007](#)].
- [30] I. Szapudi, *Wide angle redshift distortions revisited*, *Astrophys. J.* **614** (2004) 51–55, [[astro-ph/0404477](#)].
- [31] J. Yoo and U. s. Seljak, *Wide Angle Effects in Future Galaxy Surveys*, *Mon. Not. Roy. Astron. Soc.* **447** (2015) 1789–1805, [[1308.1093](#)].
- [32] E. Castorina and M. White, *Beyond the plane-parallel approximation for redshift surveys*, *Mon. Not. Roy. Astron. Soc.* **476** (2018) 4403–4417, [[1709.09730](#)].
- [33] A. Taruya, S. Saga, M.-A. Breton, Y. Rasera and T. Fujita, *Wide-angle redshift-space distortions at quasi-linear scales: cross-correlation functions from Zel’dovich approximation*, *Mon. Not. Roy. Astron. Soc.* **491** (2020) 4162–4179, [[1908.03854](#)].
- [34] E. Castorina and M. White, *Wide angle effects for peculiar velocities*, *Mon. Not. Roy. Astron. Soc.* **499** (2020) 893–905, [[1911.08353](#)].
- [35] M. Shiraishi, T. Okumura, N. S. Sugiyama and K. Akitsu, *Minimum variance estimation of galaxy power spectrum in redshift space*, *Mon. Not. Roy. Astron. Soc.* **498** (2020) L77–L81, [[2005.03438](#)].
- [36] M. Shiraishi, K. Akitsu and T. Okumura, *Alcock-Paczynski effects on wide-angle galaxy statistics*, *Phys. Rev. D* **103** (2021) 123534, [[2103.08126](#)].
- [37] M. Shiraishi, A. Taruya, T. Okumura and K. Akitsu, *Wide-angle effects on galaxy ellipticity correlations*, *Mon. Not. Roy. Astron. Soc.* **503** (2021) L6–L10, [[2012.13290](#)].
- [38] M. Shiraishi, N. S. Sugiyama and T. Okumura, *Polypolar spherical harmonic decomposition of galaxy correlators in redshift space: Toward testing cosmic rotational symmetry*, *Phys. Rev. D* **95** (2017) 063508, [[1612.02645](#)].
- [39] N. Bartolo, A. Kehagias, M. Liguori, A. Riotto, M. Shiraishi and V. Tansella, *Detecting higher spin fields through statistical anisotropy in the CMB and galaxy power spectra*, *Phys. Rev. D* **97** (2018) 023503, [[1709.05695](#)].
- [40] K. Akitsu, N. S. Sugiyama and M. Shiraishi, *Super-sample tidal modes on the celestial sphere*, *Phys. Rev. D* **100** (2019) 103515, [[1907.10591](#)].
- [41] M. Shiraishi, T. Okumura and K. Akitsu, *Minimum variance estimation of statistical anisotropy via galaxy survey*, *JCAP* **03** (2021) 039, [[2009.04355](#)].
- [42] L. Ackerman, S. M. Carroll and M. B. Wise, *Imprints of a Primordial Preferred Direction on the Microwave Background*, *Phys. Rev. D* **75** (2007) 083502, [[astro-ph/0701357](#)].
- [43] T. Okumura and A. Taruya, *Anisotropies of galaxy ellipticity correlations in real and redshift space: angular dependence in linear tidal alignment model*, *Mon. Not. Roy. Astron. Soc.* **493** (2020) L124–L128, [[1912.04118](#)].
- [44] V. Assassi, D. Baumann and F. Schmidt, *Galaxy Bias and Primordial Non-Gaussianity*, *JCAP* **12** (2015) 043, [[1510.03723](#)].
- [45] T. Okumura, U. Seljak, Z. Vlah and V. Desjacques, *Peculiar velocities in redshift space: formalism, N-body simulations and perturbation theory*, *JCAP* **05** (2014) 003, [[1312.4214](#)].
- [46] M. Shiraishi, D. Nitta, S. Yokoyama, K. Ichiki and K. Takahashi, *CMB Bispectrum from Primordial Scalar, Vector and Tensor non-Gaussianities*, *Prog. Theor. Phys.* **125** (2011) 795–813, [[1012.1079](#)].

- [47] M.-a. Watanabe, S. Kanno and J. Soda, *The Nature of Primordial Fluctuations from Anisotropic Inflation*, *Prog. Theor. Phys.* **123** (2010) 1041–1068, [[1003.0056](#)].
- [48] N. Bartolo, S. Matarrese, M. Peloso and A. Ricciardone, *Anisotropic power spectrum and bispectrum in the $f(\phi)F^2$ mechanism*, *Phys. Rev.* **D87** (2013) 023504, [[1210.3257](#)].
- [49] J. Ohashi, J. Soda and S. Tsujikawa, *Observational signatures of anisotropic inflationary models*, *JCAP* **12** (2013) 009, [[1308.4488](#)].
- [50] N. Bartolo, S. Matarrese, M. Peloso and M. Shiraishi, *Parity-violating and anisotropic correlations in pseudoscalar inflation*, *JCAP* **1501** (2015) 027, [[1411.2521](#)].
- [51] A. Naruko, E. Komatsu and M. Yamaguchi, *Anisotropic inflation reexamined: upper bound on broken rotational invariance during inflation*, *JCAP* **04** (2015) 045, [[1411.5489](#)].
- [52] N. Bartolo, S. Matarrese, M. Peloso and M. Shiraishi, *Parity-violating CMB correlators with non-decaying statistical anisotropy*, *JCAP* **1507** (2015) 039, [[1505.02193](#)].
- [53] A. A. Abolhasani, M. Akhshik, R. Emami and H. Firouzjahi, *Primordial Statistical Anisotropies: The Effective Field Theory Approach*, *JCAP* **03** (2016) 020, [[1511.03218](#)].
- [54] T. Fujita, I. Obata, T. Tanaka and S. Yokoyama, *Statistically Anisotropic Tensor Modes from Inflation*, *JCAP* **07** (2018) 023, [[1801.02778](#)].
- [55] A. Kehagias and A. Riotto, *On the Inflationary Perturbations of Massive Higher-Spin Fields*, *JCAP* **07** (2017) 046, [[1705.05834](#)].
- [56] I. Obata and T. Fujita, *Footprint of Two-Form Field: Statistical Anisotropy in Primordial Gravitational Waves*, *Phys. Rev. D* **99** (2019) 023513, [[1808.00548](#)].
- [57] N. Bartolo, S. Matarrese, M. Peloso and A. Ricciardone, *Anisotropy in solid inflation*, *JCAP* **1308** (2013) 022, [[1306.4160](#)].
- [58] N. Bartolo, M. Peloso, A. Ricciardone and C. Unal, *The expected anisotropy in solid inflation*, *JCAP* **1411** (2014) 009, [[1407.8053](#)].
- [59] K. W. Masui and U.-L. Pen, *Primordial gravity wave fossils and their use in testing inflation*, *Phys. Rev. Lett.* **105** (2010) 161302, [[1006.4181](#)].
- [60] L. Dai, D. Jeong and M. Kamionkowski, *Anisotropic imprint of long-wavelength tensor perturbations on cosmic structure*, *Phys. Rev. D* **88** (2013) 043507, [[1306.3985](#)].
- [61] F. Schmidt, E. Pajer and M. Zaldarriaga, *Large-Scale Structure and Gravitational Waves III: Tidal Effects*, *Phys. Rev. D* **89** (2014) 083507, [[1312.5616](#)].
- [62] K. Akitsu, Y. Li and T. Okumura, *Gravitational wave fossils in nonlinear regime: Halo tidal bias and intrinsic alignments from gravitational wave separate universe simulations*, *Phys. Rev. D* **107** (2023) 063531, [[2209.06226](#)].
- [63] K. Akitsu, M. Takada and Y. Li, *Large-scale tidal effect on redshift-space power spectrum in a finite-volume survey*, *Phys. Rev. D* **95** (2017) 083522, [[1611.04723](#)].
- [64] K. Akitsu and M. Takada, *Impact of large-scale tides on cosmological distortions via redshift-space power spectrum*, *Phys. Rev. D* **97** (2018) 063527, [[1711.00012](#)].
- [65] Y. Li, M. Schmittfull and U. s. Seljak, *Galaxy power-spectrum responses and redshift-space super-sample effect*, *JCAP* **02** (2018) 022, [[1711.00018](#)].
- [66] C.-T. Chiang and A. z. Slosar, *Power spectrum in the presence of large-scale overdensity and tidal fields: breaking azimuthal symmetry*, *JCAP* **07** (2018) 049, [[1804.02753](#)].
- [67] F. Schmidt and D. Jeong, *Cosmic Rulers*, *Phys. Rev. D* **86** (2012) 083527, [[1204.3625](#)].
- [68] M. Biagetti and G. Orlando, *Primordial Gravitational Waves from Galaxy Intrinsic Alignments*, *JCAP* **07** (2020) 005, [[2001.05930](#)].

- [69] T. Okumura, A. Taruya and T. Nishimichi, *Testing tidal alignment models for anisotropic correlations of halo ellipticities with N-body simulations*, *Mon. Not. Roy. Astron. Soc.* **494** (2020) 694–702, [[2001.05302](#)].
- [70] M. Houtput and J. Tempere, *Revisiting the Maxwell multipoles for vectorized angular functions*, *arXiv e-prints* (Oct., 2021) [arXiv:2110.06732](#), [[2110.06732](#)].
- [71] J.-H. Ee, D.-W. Jung, U.-R. Kim and J. Lee, *Combinatorics in tensor integral reduction*, *Eur. J. Phys.* **38** (2017) 025801, [[1701.04549](#)].